

Review

# Using Deep Eutectic Solvent-Assisted Plating Baths to Electrodeposit Composite Coatings: A Review

Vyacheslav Protsenko 

Ukrainian State University of Chemical Technology, Nauky Ave., 8, 49005 Dnipro, Ukraine; vprotsenko7@gmail.com; Tel.: +380-567753804

**Abstract:** This review provides a systematic analysis of the literature data on the electrodeposition of composite coatings using plating baths based on a new generation of room-temperature ionic liquids known as deep eutectic solvents (DESs). Such systems offer several advantages over traditionally used aqueous electrolytes and organic solvent-based electrolytes. The colloidal–chemical properties of suspension and colloidal electrolytes for composite deposition are thoroughly examined. New theories describing the kinetics of the co-deposition of composite layers are characterized. The kinetics and mechanisms of electrochemical deposition processes of composite coatings with metallic matrices are discussed. Case studies regarding the electrodeposition of composite coatings based on electrodeposited copper, silver, zinc, tin, nickel, cobalt, and chromium from DES-assisted electroplating baths are described and systematized. The main prospective directions for further research in the discussed scientific area are highlighted.

**Keywords:** coating; electrodeposition; composite coating; deep eutectic solvent; kinetic; mechanism; properties



**Citation:** Protsenko, V. Using Deep Eutectic Solvent-Assisted Plating Baths to Electrodeposit Composite Coatings: A Review. *Coatings* **2024**, *14*, 375. <https://doi.org/10.3390/coatings14040375>

Academic Editors: Jose Maria De Teresa, Ricardo Lopez Anton and Sion Federico Olive Méndez

Received: 24 February 2024

Revised: 15 March 2024

Accepted: 21 March 2024

Published: 22 March 2024



**Copyright:** © 2024 by the author. Licensee MDPI, Basel, Switzerland. This article is an open access article distributed under the terms and conditions of the Creative Commons Attribution (CC BY) license (<https://creativecommons.org/licenses/by/4.0/>).

## 1. Introduction

Electrodeposition, as a versatile and extensively utilized method in materials science and surface engineering, holds a central position in tailoring the properties of coatings for diverse applications [1–3]. Within the broad spectrum of electrodeposited coatings, composite coatings have attracted considerable interest because of their unique combination of physicochemical and service properties [4–8].

The fabrication of composite coatings involves the simultaneous electrodeposition of a metallic matrix and dispersed particles of various sizes and chemical compositions from colloidal or suspension plating baths. Once incorporated into the metallic electrodeposited matrix, these dispersed particles enhance different properties, such as corrosion resistance, hardness, and wear resistance, and can introduce novel functional characteristics to the coatings (such as superhydrophobicity; catalytic, electrocatalytic, and photocatalytic activity; self-cleaning capability; etc.). Over recent decades, the emergence of nanostructured materials has been facilitated by electrodeposition techniques, providing avenues for a wide range of nanomaterials, including nanostructured composites [6]. Extensive research efforts have been directed towards creating mechanically strengthened composite layers, improving the magnetic properties of storage devices, decreasing electrical resistance in electronic equipment, and exploring other prospects [4–7].

It is important to highlight that the creation of composite coatings via the electrodeposition technique is limited by the requirement for conductive substrates. Conversely, the electrodeposition method offers several evident benefits, including a relatively uniform dispersion of particles across the coating's thickness, a notably rapid deposition rate, and a low operational temperature (typically below 100 °C), which is markedly lower compared to pyrometallurgical or powder metallurgy approaches. Thus, the electrodeposition method provides a simpler and more accurate means of controlling the microstructure and chemical composition of produced composite films.

Despite the significant attention given to this field, the current processes of composite electrodeposition remain imperfect, requiring ongoing refinement and further development. Specifically, it should be noted that the majority of publications on this topic have focused on suspension and colloidal deposition baths for the formation of composite layers using aqueous solutions [4–8]. However, aqueous solutions have their limitations; they are prone to rapid aggregation and sedimentation processes, which compromise the stability of the bath composition and impede the electrodeposition of composite coatings. One potential solution to this issue is the adoption of non-aqueous plating baths, specifically with solutions based on the so-called deep eutectic solvents that show particular promise in addressing these challenges.

Deep eutectic solvents, which consist of a hydrogen bond donor and acceptor, have emerged as eco-friendly alternatives to traditional electrolytes due to their minimal toxicity, biodegradability, and broad electrochemical stability range [9–17]. With their distinctive characteristics, deep eutectic solvents offer an exciting opportunity to improve the electrodeposition of composite coatings. One significant advantage of deep eutectic solvents is their dual role as solvents and electrolytes, providing a versatile environment for electrodeposition. The interaction between the components of the DES and the metal ions in the plating electrolyte influences the nucleation, growth, and morphological patterns of the electrodeposited coatings. Understanding these interactions is essential for customizing the properties of composite coatings for specific applications.

A unique characteristic of DESs as solvents is their ability to undergo the extremely flexible control and modification of their composition, defining the tunability of their physicochemical properties [9–11,18]. This feature allows for finely modulating electrodeposition performance, which is important in the production of composite coatings.

Additionally, the environmental impact of electrodeposition processes using DES-based plating baths is a crucial consideration [19,20]. The sustainable and environmentally friendly nature of DESs corresponds well with the increasing demand for green technologies. Reductions in hazardous waste and energy consumption in the electrodeposition process contribute to the vital task of sustainable production.

Up to this point, there have been published reviews dedicated to the electrodeposition of functional coatings using DES-assisted plating baths [14–17,21,22]. However, there is currently a gap in the existing literature regarding a review of publications focusing on the deposition of composite coatings using electrolytes based on DESs. The only exception is [23]. However, this review is somewhat outdated as, since its publication, some new studies have emerged thoroughly and comprehensively examining new aspects of the discussed scientific topic. Taking this into account, this review delves into various aspects of electrochemical deposition using DES-based plating baths, encompassing the impacts of bath composition, deposition parameters, and the resulting microstructure and properties of composite coatings. Additionally, an examination of recent research efforts and advancements in the field provides insights into the current state of understanding and future directions. By elucidating the complexities of electrodeposition utilizing electroplating baths containing deep eutectic solvents, this review aims to contribute to the evolving field of sustainable and efficient electroplating technologies. This review endeavors to navigate through the primary advancements, obstacles, and potential of composite coatings fabricated through the electrodeposition technique using DES-based plating baths.

## **2. Physicochemical Aspects of DES-Based Systems, Kinetics of Electrochemical Processes, and Their Impact on Composite Electrodeposition**

### *2.1. Colloidal–Chemical Stability of Plating Baths Based on DESs*

A specific and inherent characteristic of suspension and colloidal electrolytes used for the electrodeposition of composite coatings is their aggregative and sedimentation instability. In hydrophobic sols and suspensions, particle aggregation (coagulation) of the dispersed phase inevitably occurs due to excess surface energy. As a result, the particles increase in size and then in sediment. All of these are highly undesirable phenomena as they

lead to the destruction of the suspension (colloidal) electrolyte, resulting in the instability of the electrodeposition process and deteriorating the functional properties of the formed composite layers. Thus, two main types of stability of colloidal electrolytes are considered: (1) sedimentation stability, which is related to the ability of the dispersed system to resist the sedimentation of particles under the influence of a gravitational field, and (2) aggregative stability, which is the result of the system's ability to resist the aggregation (coagulation) of particles of the dispersed phase. To prevent coagulation and sedimentation, flexible tuning of the electrolyte's chemical composition is typically employed, along with the addition of surfactants and water-soluble polymers and the vigorous stirring of the solutions [6,7].

In their pioneer study [24], Abbott et al. demonstrated a significant advantage of DESs in composite electroplating processes: the stability of particulate suspensions over extended periods, surpassing both aqueous and traditional organic solvent-based baths. This advantage likely stems from a combination of factors, including the higher viscosity of the neat liquid compared to water and the Coulombic screening of surface charge by the ionic liquid, leading to a higher ionic strength. As evident from the data in Table 1, although the density of DESs differs minimally from that of concentrated aqueous electrolytes, their viscosity typically exceeds that of water solutions by 2–4 orders of magnitude (and, in some cases, even more).

**Table 1.** Viscosity and density of some DESs (based on data from [10]).

Constituents of DES		Salt:Hydrogen Bond Donor Molar Ratio	Viscosity, cP	Density, g/cm <sup>3</sup> (25 °C)
Salt	Hydrogen Bond Donor			
ChCl	urea	1:2	750 (25 °C)	1.25
ChCl	urea	1:2	169 (40 °C)	
ChCl	ethylene glycol	1:2	36 (20 °C)	
ChCl	ethylene glycol	1:2	37 (25 °C)	1.12
ChCl	ethylene glycol	1:3	19 (20 °C)	1.12
ChCl	ethylene glycol	1:4	19 (20 °C)	
ChCl	glucose	1:1	34,400 (50 °C)	
ChCl	glycerol	1:2	376 (20 °C)	1.18
ChCl	glycerol	1:2	259 (25 °C)	
ChCl	glycerol	1:3	450 (20 °C)	1.20
ChCl	glycerol	1:4	503 (20 °C)	
ChCl	1,4-butanediol	1:3	140 (20 °C)	
ChCl	1,4-butanediol	1:4	88 (20 °C)	
ChCl	CF <sub>3</sub> CONH <sub>2</sub>	1:2	77 (40 °C)	1.342
ChCl	ZnCl <sub>2</sub>	1:2	85,000 (25 °C)	
ChCl	xylitol	1:1	5230 (30 °C)	
ChCl	sorbitol	1:1	12,730 (30 °C)	
ChCl	malonic acid	1:2	1124 (25 °C)	1.25
ZnCl <sub>2</sub>	urea	1:3.5	11,340 (25 °C)	1.63

As stated in [25], the coagulation rate constant,  $K$ , can be expressed by the following equation:

$$K = \frac{4k_B T}{3\eta W} \quad (1)$$

where  $k_B$  is the Boltzmann constant,  $T$  is the absolute temperature,  $\eta$  is the viscosity of the medium, and  $W$  is the stability ratio.

If the stability ratio  $W$  equals unity,  $K$  precisely coincides with the coagulation rate constant formulated by Smoluchowski for particles that experience no interaction apart from the adhesive force upon contact [26]. Therefore,  $1/W$  serves as an indicator of the deviation from the Smoluchowski coagulation rate.  $W$  is recognized for factoring in the interactions between particles: the interplay resulting from interparticle potentials and

the hydrodynamic interaction that prevents the viscous fluid from interposing between colliding particulates.

Analysis of Equation (1) indicates that the high viscosity of electrolytes based on DESs, which exceeds the viscosity of typical aqueous solutions by several orders of magnitude, should result in extremely low values of the coagulation rate constant. Thus, the high colloidal stability of DES-based solutions compared to water systems is primarily ensured by a kinetic factor, namely, the hydrodynamic resistance of the dispersion medium in the gaps between particles [26]. However, perhaps an equally powerful stabilization factor for colloidal systems in the case of DESs, which are a type of ionic liquid characterized by high ionic strength, is the electrostatic components of disjoining pressure. This component is attributed to the electrostatic repulsion between diffuse parts of electrical double layers. According to the DLVO theory, increased ionic strength should lead to a rise in the disjoining pressure and the height of the maximum on the potential interaction curve. The presence of a noticeable electric charge on the surface of dispersed particles, resulting from the formation of a double electric layer, promotes repulsive interactions and significantly reduces the rate of coagulation. Another stabilizing factor for DES-based colloidal systems is the structural–mechanical barrier, which is realized by the formation of viscous and dense surface layers of the dispersion medium on the particle surfaces, preventing particle agglomeration [26]. Formally, this effect implies a reduction in the value of  $W$  in Equation (1). Finally, in a number of cases, the stabilization of colloidal systems with DES dispersion media can be achieved through an adsorption–solvation mechanism: the adsorption of surfactants on particle surfaces and the formation of solvation layers result in a decrease in surface energy, leading to a weakening of the aggregation tendency.

In coarse dispersion systems, instability can manifest as rapid particle sedimentation and subsequent suspension breakdown. The sedimentation rate in a gravitational field is determined by the below equation [26]:

$$v = \frac{2r^2(\rho - \rho_0)g}{9\eta} \quad (2)$$

where  $r$  is the particle radius,  $\rho$  is the density of the dispersed phase,  $\rho_0$  is the density of the dispersion medium,  $g$  is the acceleration of gravity, and  $\eta$  is the viscosity of the dispersion medium.

It is evident that the significantly higher viscosity of suspension solutions based on DESs compared to aqueous electrolytes, according to Equation (2), results in a reduction in the sedimentation rate by several orders of magnitude. As a result, in such suspensions, a highly uniform distribution of particles throughout the volume is maintained for an extended period, which promotes a more stable and productive electrodeposition of composite coatings.

Thus, utilizing DES-based electrolytes enhances the aggregative stability of colloidal systems utilized for electrodeposited composite films. For instance, while Ni–PTFE (polytetrafluoroethylene) composites can be produced from aqueous plating baths only in the presence of certain nonionic or cationic wetting agents, these coatings can be readily obtained in a DES-containing bath without any stabilizing additives as the PTFE particles disperse well in the electrolyte, without requiring wetting agents [27]. Better dispersion of the PTFE particles has been observed in the DES system compared to the water system.

Given their capacity to mitigate nanoparticle agglomeration within the electroplating bath, deep eutectic solvents enable higher nanoparticle loading in the metal matrix compared to aqueous solutions [28]. This effect has been attributed to the diminished hydration force between SiO<sub>2</sub> particles and the non-aqueous electrolyte [29].

The addition of nano- and micro-sized particles to DESs has a significant impact on the colloidal–chemical and rheological characteristics of these fluids. In certain instances, unexpected phenomena have been observed that lack clear and definitive theoretical explanations. For example, when micron-sized particles (such as SiC) were introduced into ionic liquids containing copper salt, a decrease in viscosity was observed in specific

concentration ranges [24]. This observation was unexpected, prompting the authors to propose explanations centered around an increase in the fluid's free volume and localized solvent perturbations, where particles functioned as microstirrers within the liquid.

## 2.2. Kinetics and Mechanisms of Composite Coating Deposition Using DESs

The systematic progress in the electrochemical deposition of composite coatings, including processes utilizing DES-assisted plating baths, requires the development of a suitable kinetic model to understand this complex phenomenon. Various theories have been proposed to elucidate the incorporation of inert particles into growing metal films [6].

For example, Guglielmi [30] proposed a model that describes the integration of particles into a metal matrix as a two-step process of adsorption. In the initial stage, known as "loose adsorption", dispersed particles hosting adsorbed ionic constituents of the electrolyte (primarily ions of the deposited metal) and solvate shells undergo reversible adsorption on the electrode surface, resulting in relatively high surface coverage. According to Guglielmi's model, this stage is primarily of a physical nature. The subsequent stage involves the irreversible "strong adsorption" of dispersed particles, induced by the reduction in metal ions adsorbed on the particle surface. Subsequently, the particles become trapped by the growing metal matrix. This second adsorption stage is believed to have an electrochemical nature. Guglielmi suggested that the loose adsorption of dispersed particles in the first stage is reversible and, therefore, the degree of surface coverage due to loose adsorption can be described using the classical Langmuir adsorption isotherm.

Although Guglielmi's kinetic model of coating co-deposition has gained acceptance and validation from researchers [6,7], it is crucial to acknowledge that this theory is not flawless and has several shortcomings. One of the key drawbacks of this theory is that a physical model integrating both the reversible and the irreversible adsorption of particles of the same nature on the same surface seems inherently contradictory and overly complex and lacks strong substantiation. The assumption of the a priori reversible nature of the adsorption of dispersed particles in the initial stage of the process is made without accompanying evidence.

Despite numerous efforts to develop improved kinetic models for the electrodeposition of composite coatings [31–39], most current models still have shortcomings [7]. It is worth noting that nearly all previously proposed theories in this area either explicitly or implicitly assume that the adsorption of dispersed particles on a growing metal surface is reversible. However, it is well established that the adsorption of dispersed particles on solid surfaces tends to be irreversible [40–42], a critical aspect often neglected in many theoretical models aimed at describing the kinetics of the electrodeposition of composite coatings.

To address this concern, ref. [43] introduced a novel kinetic model for the electrodeposition of composite coatings based on the assumption of the irreversible adsorption of dispersed particles onto the electrode surface. This theoretical concept suggests that the amount of dispersed phase incorporated into the electrodeposited composite coating is determined by the kinetics of the irreversible adsorption stage. The key difference between the kinetic model developed in [43] and Guglielmi's theory is illustrated in Figure 1. Guglielmi's model suggests that the adsorption/desorption processes of dispersed particles occur rapidly, reaching equilibrium surface coverage primarily through loose adsorption (Figure 1a). However, only a small fraction of these adsorbed particles are subsequently integrated into the composite coatings via strong adsorption. In contrast, the proposed model suggests that the steady-state surface concentration of dispersed particles is controlled by the rate of two processes: the fixation of particles on the surface through irreversible adsorption and their subsequent removal from the surface through incorporation into the deposit as they become part of the metal matrix (Figure 1b).

In [43], the following equation was proposed to describe the co-deposition process of composite coatings and determine certain process parameters:

$$\frac{1}{\alpha} = \frac{6q_{Me}i}{kC_0\pi\rho_{Me}d^3} + \frac{1}{\alpha_{max}} \quad (3)$$

where  $\alpha$  is the degree of surface coverage with adsorbed particles,  $\alpha_{\max}$  is the maximum degree of surface coverage,  $k$  is the adsorption rate constant,  $C_0$  is the concentration of dispersed particles in the electrolyte volume,  $i$  is the partial current density of metal deposition,  $q_{Me}$  is the electrochemical equivalent of the metal,  $\rho_{Me}$  is the density of the metal, and  $d$  is the diameter of particles.

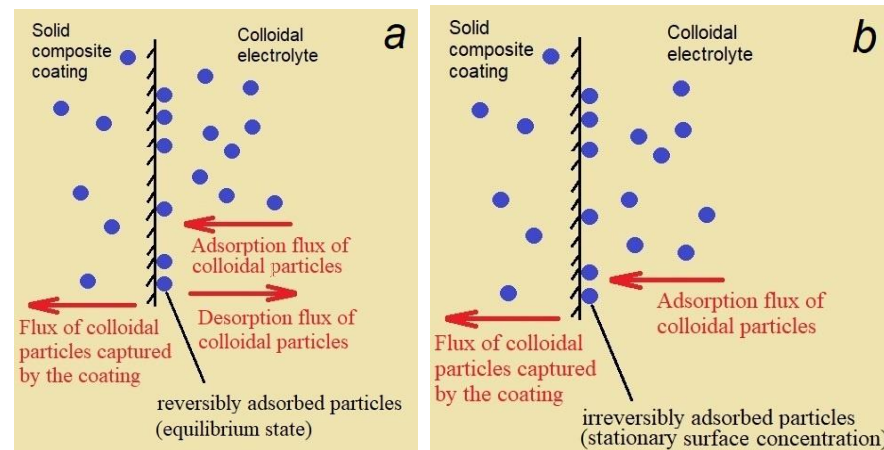


**Figure 1.** Schematic representations illustrating the incorporation of dispersed phase particles into the composite coating based on models assuming reversible (a) and irreversible (b) adsorption of particles on a metal surface. It should be noted that the length of the arrows in (a) does not accurately represent the scale of the corresponding fluxes as the rate of reversible adsorption/desorption can be orders of magnitude higher than the rate of particle inclusion in the composite coating. Reprinted from [43], copyright 2022, with permission from Elsevier.

According to Equation (3), a graph plotted in coordinates  $\frac{1}{\alpha}$  vs.  $\frac{1}{C_0}$  should result in a straight line with an intercept at  $\frac{1}{\alpha_{\max}}$ , facilitating the determination of the value of  $\alpha_{\max}$ . The slope of this resultant straight line equals  $\frac{6q_{Me}i}{k\pi\rho_{Me}d^3}$ , enabling the calculation of the adsorption rate constant  $k$ . The suggested model in [43] was employed to interpret experimental data concerning the kinetics of the electrochemical deposition of nickel–titania composite coatings deposited using both an aqueous electrolyte and an electrolyte prepared based on a deep eutectic solvent. Plots depicted with coordinates  $\frac{1}{\alpha}$  vs.  $\frac{1}{C_0}$  for Ni–TiO<sub>2</sub> composite coatings fabricated from an electrolyte based on a DES exhibited a linear trend (Figure 2). Deviations from linearity were observable for the smallest values of  $\frac{1}{C_0}$ , corresponding to high degrees of surface coverage near the maximum, where the condition  $(1 - \alpha) \approx 1$ , as assumed during the derivation of Equation (3), was no longer satisfied. The values of  $k$  and  $\alpha_{\max}$  were found for various deposition current densities using Equation (3) for the linear segments of dependences in Figure 2 (Table 2).

**Table 2.** Calculated kinetic parameters regarding electrodeposition of Ni–TiO<sub>2</sub> composite coating from an electrolyte based on DES. Reprinted from [43], copyright 2022, with permission from Elsevier.

Current Density (A dm <sup>-2</sup> )	Parameter *		
	$k$ (m s <sup>-1</sup> )	$\alpha_{\max}$	$R^2$
1	$2.612 \times 10^{-6}$	0.256	0.997
1.5	$2.159 \times 10^{-6}$	0.220	0.999
2	$1.554 \times 10^{-6}$	0.158	0.999
3	$1.520 \times 10^{-6}$	0.093	0.998

\* Note:  $R^2$  stands for the calculated coefficients of determination.

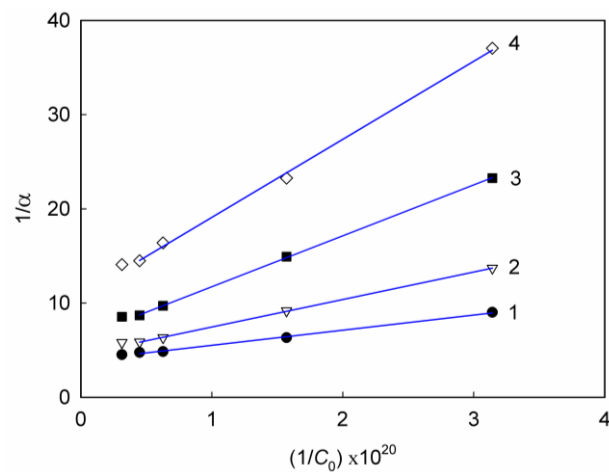


**Figure 2.** Relationships plotted in linear coordinates of Equation (3) for deposition of Ni–TiO<sub>2</sub> composite coatings using a DES-based electrolyte. Electrodeposition current density (A dm<sup>−2</sup>): (1) 1; (2) 1.5; (3) 2; and (4) 3. Reprinted from [43], copyright 2022, with permission from Elsevier.

While the adsorption rate constants for the incorporation of titania particles into the nickel matrix deposited remained relatively consistent for both the aqueous electrolyte and the DES-based electrolyte (approximately 10<sup>−6</sup> m s<sup>−1</sup>), the value of  $k$  was notably higher for the DES-based electrolyte under similar conditions [43]. For instance, at a current density of 2 A dm<sup>−2</sup>, the adsorption rate constants were 0.453 × 10<sup>−6</sup> m s<sup>−1</sup> and 1.554 × 10<sup>−6</sup> m s<sup>−1</sup> for coatings deposited using an aqueous solution and a deep eutectic solvent, respectively. This disparity was attributed to the different sizes of titania particles used. Nanoscale particles, such as Degussa P 25, exhibit higher surface energy compared to submicron-sized particles. Under specific circumstances, this heightened surface energy may contribute to the formation of a stronger adhesive bond with the surface of the deposited matrix, resulting in an increased adsorption rate constant. This phenomenon is likely linked to the observation that composites obtained from the DES-based electrolyte incorporate a significantly larger amount of the TiO<sub>2</sub> phase compared to coatings from an aqueous electrolyte (at comparable mass concentrations of the dispersed phase in the electrolytes under consideration), and they exhibit higher values of  $\alpha_{\max}$ .

The relationship between the adsorption rate constant and current density revealed a significant distinction between the two electrolyte types under consideration [43]. For the aqueous electrolyte, an elevation in current density (essentially, an increase in cathode polarization) corresponded to a rise in the value of  $k$ . Conversely, for the DES-based electrolyte, an increase in current density led to a decrease in  $k$ . This observed effect was presumed to stem from notable differences in the structure of the electric double layer in aqueous and DES-based electrolytes [44,45].

Mamme et al. [45] showed that in DES-based systems, the double layer exhibits a sophisticated cluster structure comprising multiple adsorption layers, each enriched with specific molecular or ionic components from the solution. The structure and composition of these layers are notably influenced by the electric charge of the electrode. On a negatively charged electrode surface, two layers form, enriched with hydrogen bond donor molecules arranged differently in relation to the electrode surface. It was postulated [43] that the emergence of multiple layers containing ionic and molecular components within the double layer (essentially, its structural complexity) with an increase in the cathode polarization hampers the complete or partial disruption of adsorption layers and solvate shells. This hindrance serves as a prerequisite for the irreversible adsorption of dispersed particles onto the surface of the growing nickel layer and the formation of a strong adhesive bond. Ultimately, this phenomenon resulted in the observed reduction in the adsorption rate constant with an increase in cathode current density (Table 2).

A comparison of data regarding the incorporation of titania nanoparticles into the nickel electrodeposited matrix in aqueous solutions and DES-based plating baths revealed [46] that the DES-assisted system offers a relatively lower TiO<sub>2</sub> content compared to water solutions under otherwise similar conditions. In particular, it was noted that the maximum TiO<sub>2</sub> content reaches 2.35 wt.% and 11.58 wt.% when using DES-assisted electrolytes (without the addition of water) and aqueous electrolytes, respectively. This observation was elucidated through the following rationale. Each particle suspended in a plating bath is enveloped by a thin layer of the electrolyte, which must be removed to be integrated into the growing metal electrodeposit. Likewise, a thin layer of electrolyte components should be removed from the electrode surface during the entrapment of particles into the depositing matrix. This process also encompasses the potential presence of adsorbed layers on the electrode that necessitate partial or complete disruption. It is imperative to consider that DES-containing electrolytes diverge from aqueous counterparts due to significantly higher viscosity and density. Consequently, DES-based systems necessitate substantially more time and energy to destroy dense and viscous films formed on the surfaces of both particles and a growing metal matrix, impeding the rate of particle inclusion into deposits and thereby diminishing the maximum available content of an inert dispersed phase in the deposited composite layer.

At the same time, the physicochemical properties of DESs can be finely tuned by the addition of water, which, in this case, serves not only as a solvent but also as an additional special hydrogen bond donor [47]. It has been demonstrated [48] that the addition of water to a colloidal electrolyte results in a significant decrease in viscosity, facilitating the easier disruption of surface layers. Furthermore, the reduction in electrolyte viscosity accelerates the transfer of colloidal particles to the electrode surface. These phenomena account for the observed increase in TiO<sub>2</sub> content when water is introduced into the electrolyte. However, once a certain threshold value is reached, the TiO<sub>2</sub> content in the composite coating remains constant regardless of the water content [48]. It is understood that a certain “burial time” is necessary for a colloidal particle adsorbed on the surface to become entrapped in a growing metal matrix [36]. An adsorbed particle can only be integrated into a composite if its “residence time” exceeds the “burial time”. It seems that the residence time begins to decrease at a certain level of added water due to the accelerated desorption of particles caused by the competitive adsorption of water molecules on the surface of hydrophilic nickel. Consequently, the TiO<sub>2</sub> content in composite coatings stops increasing.

It has been demonstrated [24] that the co-deposition of electrochemically inert particles of the dispersed phase affects the kinetics of electrochemical deposition of the metal matrix. Specifically, the cyclic voltammograms registered during the electrodeposition of copper from DES-assisted plating baths with 10 wt.% Al<sub>2</sub>O<sub>3</sub> or SiC (Figure 3) indicate a significant decrease in current upon the addition of particulates to the solution. Analysis of the data led to the conclusion that the observed reduction in the current can be explained by the physical blocking of the electrode surface by the non-conductive particulate matter, thereby effectively diminishing the conductive area of the electrode surface. Additionally, Figure 3 illustrates some variation in peak potentials corresponding to the different types of deposits, particularly noticeable in the anodic stripping response. This variability is expected as the peak position is influenced by the timescale; therefore, the copper components in different composites will be electrochemically dissolved at a rate that is sensible for the composite composition.

In [24], the consistent kinetic stability of solutions based on a DES throughout the experimental period was underscored, indicating the absence of the settling of Al<sub>2</sub>O<sub>3</sub> particles. This implies that the sedimentation of alumina particles did not significantly affect their overall incorporation rate. It was presumed that the principal mechanism governing the inclusion of particles into the deposited metal matrix was the irreversible adsorption mechanism discussed earlier. Moreover, it was noted that larger particles were more effectively incorporated at lower solution concentrations, while both particle sizes exhibited preferential distribution into the metal deposit at higher concentrations.

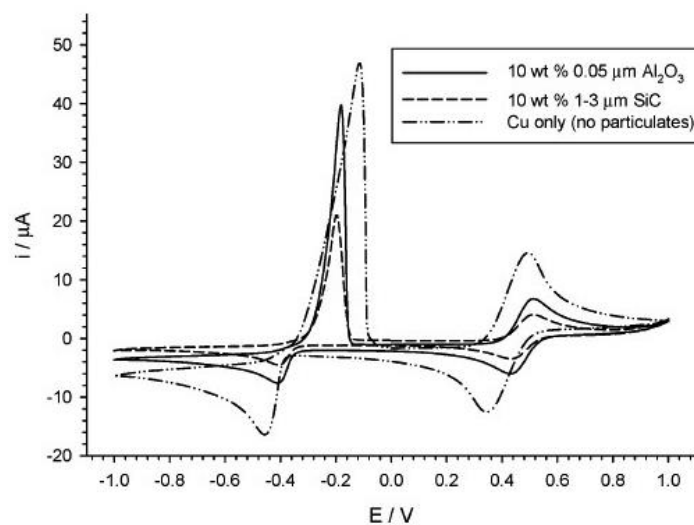


**Figure 3.** Voltammograms registered on platinum working electrode in electrolyte containing  $0.02 \text{ mol dm}^{-3} \text{ CuCl}_2 \cdot 2\text{H}_2\text{O}$  dissolved in deep eutectic solvent (eutectic mixture of ethylene glycol and choline chloride with the addition of either 10 wt.%  $\text{Al}_2\text{O}_3$  or SiC. Potential sweep was  $0.010 \text{ V s}^{-1}$ ; silver wire was used as quasi-reference electrode. Reprinted from [24], copyright 2009, with permission from Royal Society of Chemistry.

The addition of  $\text{SiO}_2$  nanoparticles into a DES-based solution containing dissolved Ni(II) salt was observed to alter the response of cyclic voltammetry [28]. Specifically, the peak potential of Ni(II) ion electroreduction shifted towards more positive values, accompanied by an increase in maximum current density upon the introduction of  $\text{SiO}_2$  nanoparticles into the DES. The authors proposed two potential roles of  $\text{SiO}_2$  particles in the electrodeposition process. Firstly, active  $\text{SiO}_2$  particles may serve as efficient preferential nucleation sites, thereby facilitating the electrochemical deposition process. Secondly,  $\text{SiO}_2$  nanoparticles could directly take part in the electrode reaction and catalyze the electrodeposition of nickel.

The nucleation and growth processes of Ni- $\text{SiO}_2$  composite deposition were investigated through the chronoamperometry technique [29]. It was observed that the nucleation of pure nickel closely followed a three-dimensional progressive nucleation mechanism at more positive potentials, gradually transitioning to a three-dimensional instantaneous nucleation mechanism as the applied potential shifted towards more negative values. However, in the Ni- $\text{SiO}_2$  system, nucleation predominantly followed a three-dimensional instantaneous mechanism. As the concentration of  $\text{SiO}_2$  increased, the nucleation mode gradually deviated from the theoretical model. This difference in nucleation behavior between the deposition of pure nickel and Ni- $\text{SiO}_2$  composites was attributed to changes in the surface charge of particles and the thickness of the electrical double layer resulting from the presence of  $\text{SiO}_2$  nanoparticles. The observed deviations in nucleation behavior in the Ni- $\text{SiO}_2$  system were associated with the growth process, which exhibited diffusion and partial kinetic rate control. The partial kinetic control of growth may be attributed to the chemical interaction between Ni(II) ions and the unsaturated bonds of oxygen atoms on the surface of silica particles.

A comprehensive investigation into the nucleation and growth mechanism of the electrochemical deposition of Ni-SiC composites in an ethylene glycol/choline chloride-based DES containing either micro- or nano-sized SiC particles was conducted by Li et al. [49]. In the absence of added SiC particles, the nucleation of nickel typically followed the three-dimensional progressive mechanism, particularly at relatively positive applied potentials. However, as the potential shifted negatively, the nucleation mode gradually transitioned towards a three-dimensional instantaneous mechanism (Figure 4). These observations are consistent with the findings reported in [29]. However, upon introducing micro-sized SiC particles ( $0.3 \mu\text{m}$ ) into the DES plating electrolyte, the nucleation mechanism of nickel

initially aligned with three-dimensional instantaneous nucleation and then showed some deviation from the theoretical pattern. Conversely, the nucleation of nickel in the presence of nano-sized SiC particles (40 nm) closely adhered to the three-dimensional instantaneous nucleation mechanism. Thus, it can be inferred that micro- and nano-sized particles exert distinct effects on the nucleation and growth mechanism of the metal [49].

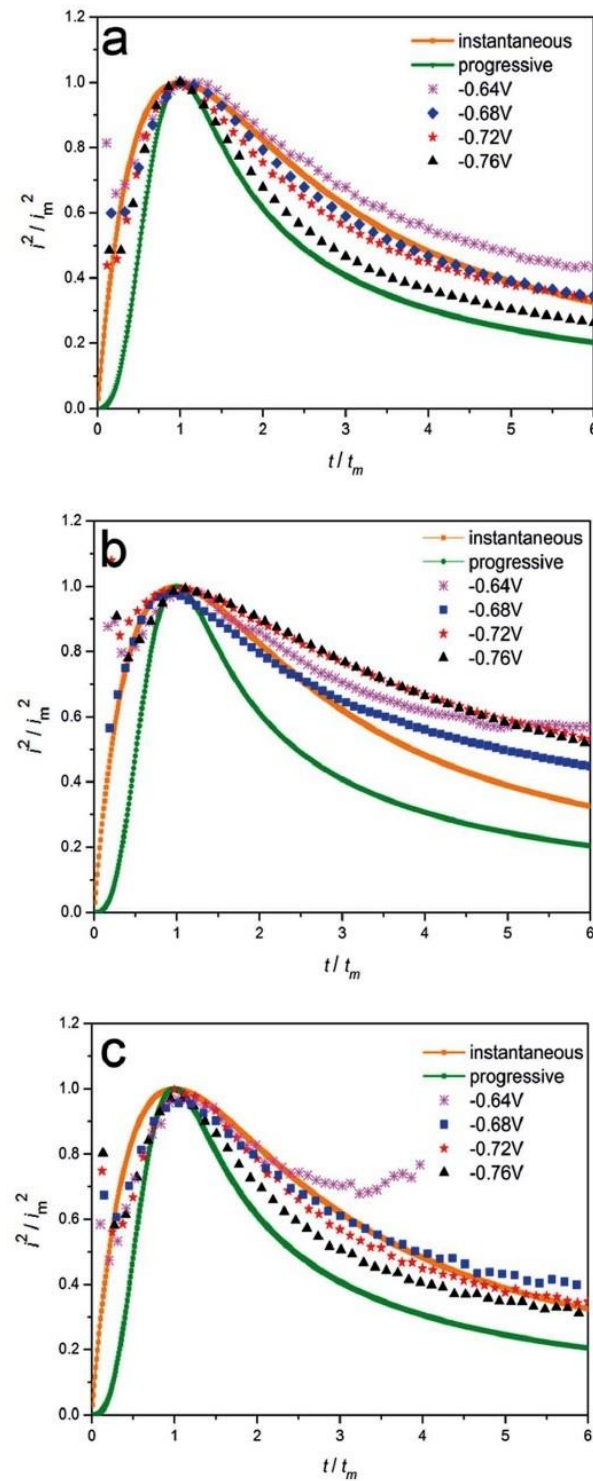


**Figure 4.** Current vs. time curves plotted in dimensionless coordinates for deposition of nickel and Ni-SiC composites: (a) without SiC particles, (b) with micro-SiC particles, and (c) with nano-SiC particles. Reprinted from [49], copyright 2015, with permission from Royal Society of Chemistry.

As evident from numerous case studies discussed below, the use of electrolytes based on DESs often yields coatings with a nanocrystalline structure [23]. This may be explained by the effect of several key factors. Firstly, DES-based solutions typically exhibit higher viscosity and density compared to aqueous electrolytes. This difference in fluid properties can slow down diffusion processes and crystal growth rates, favoring the formation of nanocrystalline structures. Secondly, DESs may have distinct effects on the kinetics of crystal growth compared to aqueous solutions due to their unique chemical properties and reactivity. Thirdly, the chemical interaction between the electrode surface and DES-based electrolytes may differ from that in aqueous solutions, influencing nucleation and crystal growth processes. Aqueous electrolytes without the addition of surfactants typically lead to the formation of microcrystalline structures due to rapid nucleation and growth processes facilitated by the high mobility of ions in the solution and rapid diffusion. However, the use of DESs can modify these conditions, slowing down surface diffusion and charge transfer and promoting the formation of nanocrystalline structures. In summary, the utilization of DES-based plating electrolytes alters the deposition conditions, leading to the formation of nanocrystalline coatings, whereas, under similar conditions, microcrystalline coatings are typically obtained from aqueous electrolytes.

### 3. Case Studies

Below, we will delve into case studies described in the literature concerning the electrodeposition of composite coatings using DES-based electrolytes, along with the characterization of the properties and potential applications of the resulting composite layers. The analysis will be structured according to a classification based on the chemical nature of the material constituting the deposited metal matrix, which is commonly used when discussing data concerning the electrochemical synthesis of composite layers.

#### 3.1. Copper-Based Composites

The study conducted by Abbott et al. [24] marked a pioneering investigation into the electrodeposition of composites using DESs based on choline chloride. The researchers explored the electrodeposition process of Cu–Al<sub>2</sub>O<sub>3</sub> and Cu–SiC composites utilizing two distinct ionic liquids: one comprising a eutectic mixture of choline chloride and ethylene glycol (commercially known as ethaline) and the other comprising a eutectic mixture of choline chloride and urea (commercially known as reline). Inert dispersed phases of alumina (with particle sizes of 0.05 μm and 1.0 μm) or silicon carbide (ranging from 1 to 3 μm) were added to the electroplating baths. The loading of Al<sub>2</sub>O<sub>3</sub> and SiC particles within the resulting electroplated films was found to be significantly influenced by the particulate concentration in the solution while remaining largely unaffected by the concentration of copper metal ions or the duration of the process. An elevation in the concentration of colloidal particles in the solution corresponded to an increase in their content within the composite electrodeposits.

An important observation from Abbott et al. [24] is that at lower solution concentrations, larger particles exhibited a more efficient incorporation compared to smaller ones. However, at higher concentrations, both particle sizes were preferentially partitioned into the metal deposit. The primary mechanism attributed to the inclusion of particles was identified as diffusion/convection driven by the concentration gradient.

The process of the electrodeposition of Cu/nano-SiC composites from DESs based on ethylene glycol and the influence of the addition of two surfactants, sodium dodecyl sulfate and cetyl trimethyl ammonium bromide, were investigated [50]. It was observed that sodium dodecyl sulfate reduced the SiC content, while cetyl trimethyl ammonium bromide increased the loading of inert particles in the coatings. The presence of surfactants also affected the surface morphology of the composite coatings.

### 3.2. Silver-Based Composites

Abbott et al. [51] investigated the electrodeposition of a silver-based composite utilizing deep eutectic solvents comprising ethylene glycol and choline chloride for the first time. The plating electrolyte contained  $0.1 \text{ mol dm}^{-3}$  silver chloride dissolved in ethaline. The addition of nano-sized SiC particles (50 nm) did not alter the surface morphology of the silver matrix; however, it led to a doubling of the microhardness of the electrodeposited coatings. Interestingly, increasing the size of the SiC particles from 50 nm to 2  $\mu\text{m}$  did not affect the microhardness of the composites, although it did result in a significant decrease in wear volume (from  $4440 \mu\text{m}^3$  to  $4263 \mu\text{m}^3$ , respectively). This finding is noteworthy as it suggests the feasibility of depositing silver composites with enhanced wear resistance for electrical contacts using DES-assisted plating electrolytes. The inclusion of  $\text{Al}_2\text{O}_3$  nanoparticles (50 nm) had the most pronounced effect on the microhardness of the deposits; however, the wear volume and surface morphology were comparable to those of coatings containing SiC particles of the same size. Therefore, it can be concluded that the friction coefficient and wear resistance are determined by the nature rather than the size of the added particles [51].

### 3.3. Zinc-Based Composites

Marín-Sánchez et al. [52] reported the cathodic electrodeposition of Zn–cerium oxides using the deep eutectic solvent choline chloride-urea (reline). Zinc and cerium chloride salts ( $\text{ZnCl}_2$  and  $\text{CeCl}_3 \cdot 7\text{H}_2\text{O}$ ) were added to the plating electrolyte both separately ( $0.3 \text{ mol dm}^{-3}$  in each case) and jointly (at the Zn:Ce ratio of 3:1). Cerium was integrated into the electrodeposit as a mixed oxide  $\text{Ce}_2\text{O}_3 + \text{CeO}_2$  within the zinc metal matrix. The surface morphology and chemical composition of the coatings varied with the current density of the electrodeposition process. The maximum cerium content, averaging  $8.30 \pm 1.36 \text{ at.}\%$ , was attained at current densities ranging from  $1.13$  to  $0.75 \text{ A dm}^{-2}$ , with cerium predominantly existing in the form of mixed oxides:  $50.6\% \text{ Ce}_2\text{O}_3 + 49.4\% \text{ CeO}_2$ . Electrochemical corrosion tests demonstrated similar corrosion rates for all coatings. In the case of defects in the zinc–cerium oxide coating, active migration of cerium was observed, potentially augmenting the protective properties of the coating in comparison to “pure” zinc.

Li et al. [53] investigated the electrochemical deposition of zinc–graphene oxide (zinc–GO) composite coatings using a plating bath containing a eutectic mixture of urea and choline chloride. The concentration of  $\text{ZnCl}_2$  in the plating solution was  $0.2 \text{ mol dm}^{-3}$ , while the concentration of GO was  $0.05 \text{ g L}^{-1}$  or  $0.10 \text{ g L}^{-1}$ . It was observed that the graphene oxide sheets exhibited extremely good dispersion stability with this DES. GO particles, when incorporated into the growing zinc metallic matrix, served as favorable nucleation sites, thereby accelerating the electrodeposition reaction. The presence of graphene oxide significantly impacted the surface morphology and phase structure of the deposited layers. Consequently, GO particulates could effectively enhance nucleation rates, reduce the growth rates of zinc nuclei, alter the grain shape from polyhedron to granule, and refine the grain structure (Figure 5). The zinc–GO composite films demonstrated superior corrosion stability compared to pure zinc, with corrosion resistance further improving as the GO content grew.

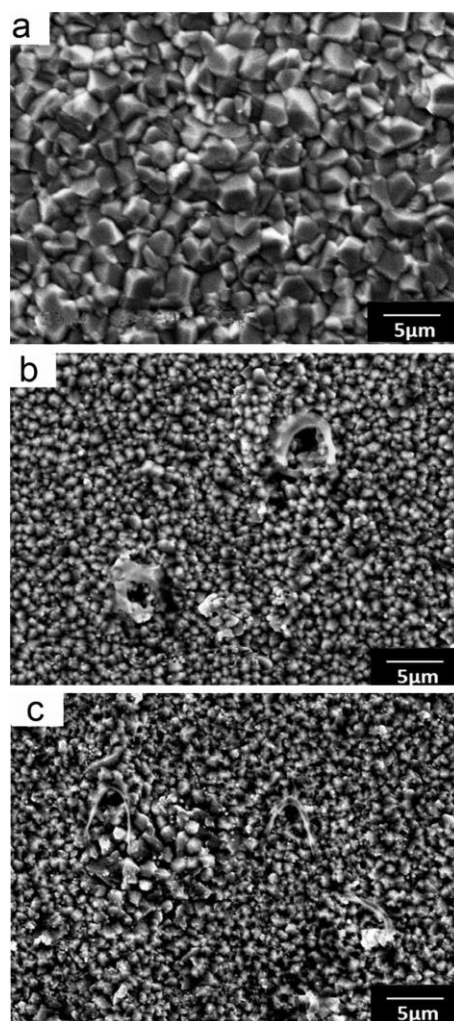


**Figure 5.** SEM micrographs depicting the surface morphology of zinc-based coatings: (a) without graphene oxide particles in the plating solution, (b) with  $0.05 \text{ g L}^{-1}$  graphene oxide, and (c) with  $0.10 \text{ g L}^{-1}$  graphene oxide. Reprinted from [53], copyright 2015, with permission from Royal Society of Chemistry.

### 3.4. Tin-Based Composites

The electrodeposition of composite coatings comprising a tin matrix with embedded reduced graphene oxide (rGO) was investigated, utilizing a deep eutectic solvent as the plating solution [54]. The electrodeposition was carried out from an ethaline-based solution, containing  $0.7 \text{ M SnCl}_2 \cdot 2\text{H}_2\text{O}$  with and without  $20 \text{ mg L}^{-1}$  rGO, at a temperature of  $70 \text{ }^\circ\text{C}$  under constant magnetic stirring. It was demonstrated that this electrolytic medium facilitated the creation of a stable and uniformly dispersed graphene oxide solution, enabling the subsequent integration of rGO sheets into the Sn matrix. The deposition process of Sn-rGO composites involved nucleation and three-dimensional growth controlled by diffusion, with nucleation transitioning from progressive to instantaneous as the overpotential increased. Uniform Sn-rGO composite films were successfully electrodeposited, demonstrating good adhesion to the copper substrate. X-ray diffraction analysis revealed that the presence of rGO in the coatings reduced the preferred orientation of tin growth along the planes (101), (211), (301), and (112). The average crystallite sizes ranged from 82 to 98 nm for pure tin and from 77 to 92 nm for Sn-rGO deposits. An enhancement in corrosion resistance was observed for the Sn-rGO composite films compared to pure tin. Furthermore, the results indicated satisfactory solderability of the coatings, indicating that

the electrochemically deposited Sn-rGO composite could serve as an efficient solder layer, as evidenced by wetting angles of about 44°.

### 3.5. Nickel-Based Composites

The majority of the published literature on composite electrodeposition using DES-based plating solutions focuses on materials with a nickel matrix. For example, Li et al. [28] proposed a method for the in situ synthesis of SiO<sub>2</sub> nanoparticles in a DES-assisted medium (ethaline), enabling the synthesis of highly dispersed SiO<sub>2</sub> nanoparticles and the electroplating of a homogeneous nickel matrix with evenly distributed silica nanoparticles. In this process, tetraethyl orthosilicate (Si(OC<sub>2</sub>H<sub>5</sub>)<sub>4</sub>) was blended with ethaline and hydrolyzed with the addition of a 10 wt.% hydrochloric acid solution. The resulting silica particles had diameters ranging from 40 to 65 nm. The amount of captured silica nanoparticles in the composite films reached 5.13 wt.%. Friction and wear tests revealed that the uniform dispersion of silica nanoparticles in the Ni matrix notably enhanced the tribological performance of the composite electrodeposited layers, leading to improved wear strength and stable coefficients of friction.

In [29], SiO<sub>2</sub> nanoparticles were co-deposited into a nickel matrix using an ethaline-based DES through pulsed electrolysis. The concentration of NiCl<sub>2</sub>·6H<sub>2</sub>O in the electrolyte was 0.2 mol dm<sup>-3</sup>, while the contents of nano-sized SiO<sub>2</sub> (15–30 nm) were 0, 5, 15, 25, 35, and 45 g/L. It was suggested that the presence of these embedded silica nanoparticles significantly influenced the nucleation and growth processes, microstructure, and chemical composition of the composite electrodeposits. The maximum content of embedded SiO<sub>2</sub> particles (approximately 4.69 wt.%) was detected in the absence of any stabilizing additives. In comparison to pure nickel coatings, the Ni–SiO<sub>2</sub> nanostructured composite coatings demonstrated notably improved corrosion resistance, with the level of enhancement correlating to the increase in the SiO<sub>2</sub> particulate loading in the electrodeposited films (Figure 6, Table 3) [29].

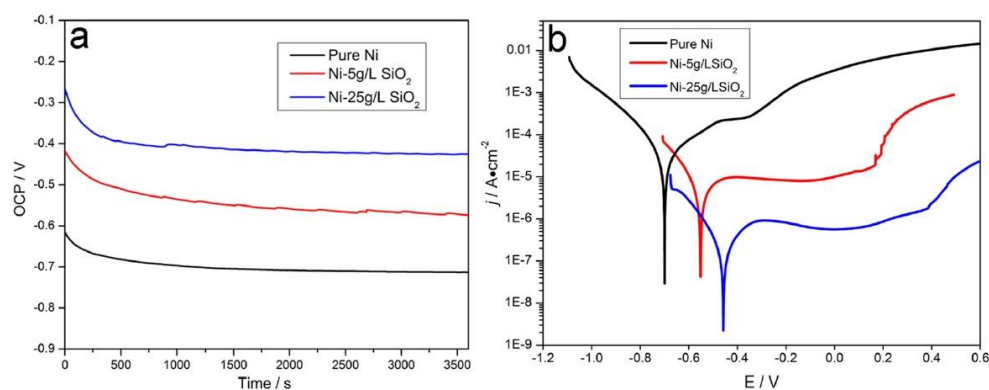


**Figure 6.** Open circuit potential (OCP) vs. time plot (a) and potentiodynamic polarization curves (b) of nickel and nickel–SiO<sub>2</sub> composite coatings recorded in 3.5% solution of NaCl. Reprinted from [29], copyright 2016, with permission from Elsevier.

**Table 3.** Parameters derived from corrosion test of nickel and nickel–SiO<sub>2</sub> composite coatings in 3.5% solution of NaCl. Reprinted from [29], copyright 2016, with permission from Elsevier.

Specimens	$E_{\text{corr}}$ (V vs. Ag/AgCl)	$i_{\text{corr}}$ (A/cm <sup>2</sup> )
Pure Ni	−0.72	$3.92 \times 10^{-5}$
Ni-5g/L SiO <sub>2</sub>	−0.57	$3.23 \times 10^{-6}$
Ni-25g/L SiO <sub>2</sub>	−0.43	$2.89 \times 10^{-7}$

Ni–SiC composite coatings were produced through a pulsed electrodeposition technique using an ethaline-based DES [49]. Silicon carbide particles of varying sizes (0.3 μm

or 40 nm) were employed in formulating the plating solutions, the contents of the micro- or nano-sized SiC particles being 5, 10, 15, 20, 25, and 30 g L<sup>-1</sup>. The electrolyte contained also 0.2 mol dm<sup>-3</sup> NiCl<sub>2</sub>·6H<sub>2</sub>O. Both nano- and micro-scale SiC particles were uniformly dispersed within the electrodeposited Ni matrix. The influences of particle concentration in the electrolyte, current density, and solution stirring rate on the silicon carbide particle content in the composite electrodeposits were investigated. The maximum loadings of nano- and micro-sized SiC dispersed phases in the composite layers were found to be up to 5.37 wt.% and 12.80 wt.%, respectively. The obtained composite films exhibited greater hardness and enhanced wear resistance compared to pure Ni coatings. Specifically, while the microhardness of pure nickel was approximately 289 HV, it increased to 895 HV and 716 HV with the introduction of nano- and micro-sized SiC particulates into the coatings, respectively [49].

Ni-PTFE composite coatings deposited via the electrodeposition method have garnered significant interest owing to their favorable properties such as low friction coefficient, solid lubrication, and excellent water repellency. Research by You et al. [27] introduced a deep eutectic solvent-based bath for electrodepositing Ni-PTFE composite layers, eliminating the need for wetting agents. Thus, the electrolyte contained 1.0 mol dm<sup>-3</sup> NiCl<sub>2</sub>·6H<sub>2</sub>O in ethaline and the concentration of PTFE particles was 5 or 10 g L<sup>-1</sup>. The obtained coatings contained approximately 3 wt.% of PTFE. The incorporation of PTFE contributed to the improved wear resistance of the composites compared to pure nickel coatings. However, contrary to expectations, potentiodynamic polarization investigations revealed that pure nickel exhibited superior anticorrosion behavior compared to the Ni-PTFE composite coatings: an increase in the PTFE content in the investigated composite films resulted in a more negative corrosion potential and higher corrosion current [27].

A series of scientific publications [43,46,48,55–57] investigated the electrochemical deposition behavior of Ni-TiO<sub>2</sub> composite coatings using plating baths formulated with deep eutectic solvents. Furthermore, various properties of the resulting coatings were characterized. Nickel-TiO<sub>2</sub> composite coatings, deposited from DES-based electrolytes without any specific additives, contained titania particles in concentrations not exceeding 2.35 wt.% [46]. As indicated by the data presented in Figure 7, an increase in the water content in the plating electrolyte notably elevated the concentration of the titania particles in the composite films (up to ≈10 wt.%) [55].

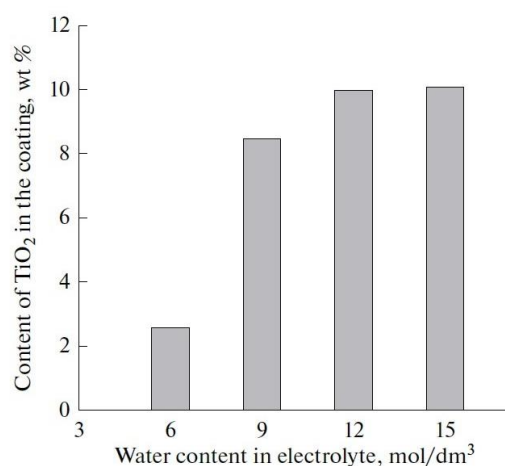


**Figure 7.** Influence of water concentration in the electrolyte on the TiO<sub>2</sub> content in electrodeposited composite layers. Current density was 1 A dm<sup>-2</sup>. Titanium dioxide particle concentration in the electrolyte was 5 g L<sup>-1</sup>. The content of Ni(II) ions in ethaline was 1 mol dm<sup>-3</sup>. Reproduced from [55], copyright 2022.

Electrodeposition using electrolytes based on DESs resulted in the formation of nanocrystalline films, with crystalline sizes ranging from approximately 6 to 10 nm, contrasting with the “typical” microcrystalline nickel obtained from aqueous nickel plating

baths [55]. This observation corroborates earlier findings [58–60], underscoring the ability to produce nanostructured nickel coatings using DES-assisted electroplating baths. Notably, the electrodeposition of nickel matrices in deep eutectic solvents proceeds under conditions of strong adsorption of both organic and inorganic components of the plating solution on the Ni surface. This phenomenon impedes surface diffusion, slows down crystallite growth rates, and ultimately facilitates the deposition of nanostructured coatings. Moreover, not only do organic components of DESs contribute to this effect but dispersed TiO<sub>2</sub> nanoparticles can also act as specific surfactants impeding the rate of Ni electrodeposition [55].

It was revealed that the incorporation of TiO<sub>2</sub> nanoparticles into a nickel matrix, along with an augmentation in their concentration within the electrodeposits, induces a shift in corrosion potential towards more positive values, an enhancement in polarization resistance, and a reduction in corrosion current density [56]. The improvement in the corrosion resistance of the coatings was attributed to the barrier effect exerted by the dispersed phase particulates and the creation of corrosion microcells, which promoted the deceleration of localized corrosion.

The electrocatalytic activity of nickel coatings and electrodeposited Ni/TiO<sub>2</sub> composites in a hydrogen evolution reaction (HER) was assessed using linear voltammetry in an alkali water electrolyte (Figure 8) [48]. Remarkably, the nickel coating fabricated with the DES-based electrolyte exhibited markedly improved electrocatalytic performance in the HER compared to the one produced from an aqueous electrolyte. This improvement was clearly observed in the polarization curve, which shifted towards more positive electrode potentials. Furthermore, the introduction of titania particles into the Ni matrix led to a shift in the polarization curve towards more positive electrode potentials, indicating an additional enhancement in electrocatalytic activity.

The findings presented in [46,48,55] suggest that the fabrication of nanostructured Ni/TiO<sub>2</sub> composite coatings using DESs holds promise for the advancement of efficient electrocatalysts in the synthesis of “green” hydrogen [61,62]. It is noteworthy that electrodeposited Ni/TiO<sub>2</sub> composite layers demonstrate not only electrocatalytic capabilities but also exhibit photocatalytic activity in the photochemical degradation of methylene blue organic dye in aqueous solutions [46]. This observation could pave the way for the development of novel heterogeneous photocatalysis processes (TiO<sub>2</sub>/UV) for wastewater treatment, leveraging electrodeposited metal matrices as reliable supports for titania particles [63,64].

Liu et al. [65] reported their investigation into the influence of boric acid and water on the deposition process of Ni–TiO<sub>2</sub> composite coatings using a deep eutectic solvent. Their findings revealed that the addition of boric acid to the plating bath yields an acidic medium, preventing the formation of hydroxide nickel(II) compounds and the decomposition of the DES constituents. Therefore, boric acid seems to be an important additive in the deposition process, particularly when employing a deep eutectic solvent-based nickel plating solution. Nevertheless, once the boric acid concentration in the composite electrolyte surpasses approximately 9 g L<sup>-1</sup>, the internal stress within the coating escalates, leading to the emergence of minor cracks in the coating structure. In addition, the introduction of extra water into the plating bath is advantageous in reducing the viscosity of the deep eutectic solvent and augmenting its conductivity. Consequently, this leads to a significant increase in the current density of nickel (II) ion electroreduction. Furthermore, water plays a crucial role in altering the complexation state of Ni(II) ions, resulting in the formation of a coating characterized by smaller crystallite dimensions. However, it is essential to note that an excessive amount of added water can facilitate the deposition of large agglomerated TiO<sub>2</sub> particles within the coating, posing potential challenges.

Several studies [66–68] have reported the electrochemical deposition of composite films that incorporate various forms of nanostructured carbon into a nickel matrix. For example, uniform nickel–multiwalled carbon nanotube (Ni–MWCNT) composite layers were fabricated using reline-based plating baths [66]. The electrolytes exhibited a remarkably stable dispersion of both initial and oxidized MWCNTs, leading to a homogeneous

distribution of MWCNTs within the deposited nickel matrix. It was observed that the crystallinity, surface morphology, roughness, and corrosion resistance of the resulting composites were directly affected by the presence of MWCNTs.

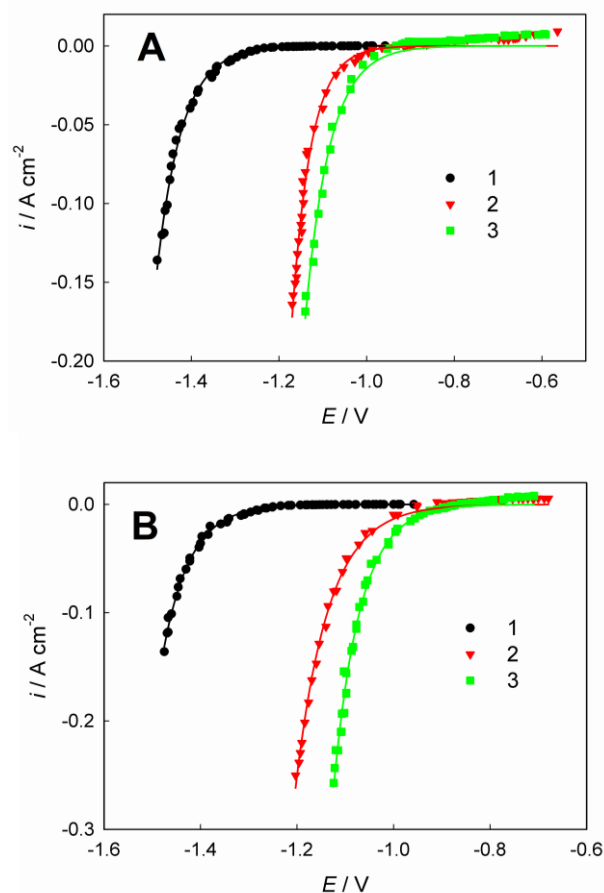


**Figure 8.** Voltammetry responses characterizing hydrogen evolution reaction on Ni (1, 2) and Ni-TiO<sub>2</sub> (3) coatings in 1 M NaOH solution at 298 K. Electrodeposition was performed using aqueous electrolytes (1) and DES-assisted plating baths (2, 3). Current density was 10 mA cm<sup>-2</sup>. The concentration of titania in the DES-based electrolytes was 5 g l<sup>-1</sup>. The DES-based baths contained (A) no extra water, and (B) 6 mol L<sup>-1</sup> extra water. The content of NiCl<sub>2</sub>·6H<sub>2</sub>O was 1 mol L<sup>-1</sup>. Reprinted from [48], copyright 2019, with permission from Elsevier.

Liu et al. [67] investigated the electrodeposition of composites with a Ni matrix using reline DES with the addition of dispersed carbon nanotubes (CNTs). The electrolyte contained 50 g L<sup>-1</sup> NiCl<sub>2</sub>·6H<sub>2</sub>O and 0.5 mol L<sup>-1</sup> CNT. The electroplated composites were found to have larger crystalline grain sizes of nickel compared to the pure deposited Ni. Moreover, the incorporation of CNTs led to an increase in surface roughness, rising from 58 nm to 94 nm following the introduction of CNTs into the coatings. The Ni-CNTs composites exhibited an exceptionally low friction coefficient and demonstrated improved tribological behavior [67]. Xiang et al. [68] addressed the challenge of graphene agglomeration in DES-assisted plating baths to synthesize graphene-reinforced composite coatings via the electrodeposition technique. The electrolyte had the following composition: 37.4 wt.% CH<sub>3</sub>CONH<sub>2</sub> (acetamide), 28 wt.% CO(NH<sub>2</sub>)<sub>2</sub> (urea), 34.6 wt.% NH<sub>4</sub>NO<sub>3</sub>, 0.05 mol L<sup>-1</sup> NiCl<sub>2</sub>·6H<sub>2</sub>O, and 30 g L<sup>-1</sup> H<sub>3</sub>BO<sub>3</sub>. The exfoliated graphene derived from the graphite anode was a source of the dispersed phase in the plating bath. The graphene content in the prepared coatings reached approximately 23.9 wt.%. The introduction of graphene did not alter the orientation of the nickel crystal faces; however, it led to a significant refinement in the grain size. The resulting composite coating exhibited exceptional microhardness compared to the pure Ni coating (Figure 9). Additionally, the composite coating demonstrated

reliable lubricating properties, with a relatively low friction coefficient (approximately 0.14) and a significantly reduced wear rate, decreased by over 60% and tenfold, respectively, in comparison to the nickel film (Figure 10).

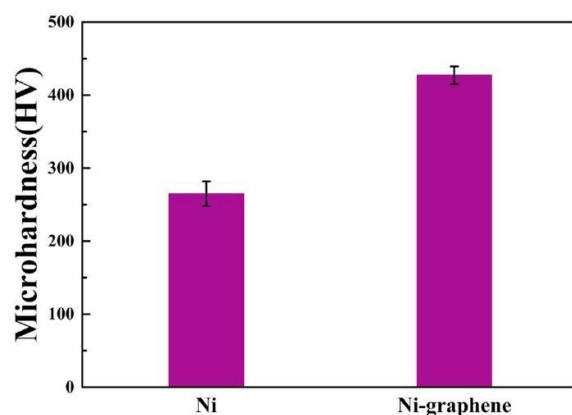


**Figure 9.** Comparison of microhardness of nickel coating and nickel–graphene composite coating. Reprinted from [68], copyright 2019, with permission from Elsevier.

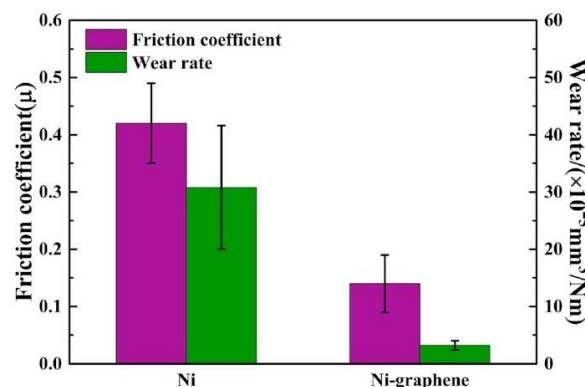


**Figure 10.** Comparison of wear rate and friction coefficient of nickel coating and nickel–graphene composite coating. Reprinted from [68], copyright 2019, with permission from Elsevier.

Wang et al. [69] investigated the electrochemical deposition of composite layers of Ni-activated carbon and Ni-nano-carbon (50 nm) in a plating electrolyte based on ethaline. The used electrolytes had the following compositions: 0.2 M  $\text{NiCl}_2 \cdot 6\text{H}_2\text{O}$  and 0, 2, 4, 6, 8, 10, 12, or 14 g  $\text{L}^{-1}$  activated carbon or 50 nm carbon particles without any pre-treatment. It was demonstrated that the electrodeposited composite coatings had a three-dimensional, flower-like microstructure. SEM images of the surface of the nickel-nano-carbon coatings (Figure 11) revealed that the carbon nanoparticles embedded within the metal matrix yielded a flower-like microstructure, reminiscent of chrysanthemums. Enhanced electrocatalytic activity towards hydrogen evolution was observed when using the electrodeposited composite as electrocatalysts. It should be noted that the variety of patterns of surface morphologies detected in [69] and illustrated in Figure 11 indicates that the electrodeposition of composite layers from electrolytes based on DESs reveals additional possibilities for controlled influence on the growth mechanism, particularly the ability to flexibly change between growth mechanisms such as “layer-by-layer”, “layer-plus-island”, and “island” growth. In traditional aqueous electrolytes, this switch between mechanisms can be achieved by varying the parameters of pulsed electrolysis [70].

A study by Cherigui et al. [71] reported the electrochemical deposition of nickel-based nanostructures onto a glassy carbon electrode using reline. It was demonstrated that the electrocatalytic hydrolysis of residual water present in the deep eutectic solvent occurred at a relatively negative electrode potential, leading to the formation of a hybrid  $\text{Ni} + \text{Ni}(\text{OH})_2$

adsorbed film. Such coatings can be viewed as composite; yet, the hydroxide particles were not directly introduced into the plating bath as a dispersed phase but rather formed in situ on the electrode surface. These electrodeposited composite layers hold significant promise for generating supported nanostructures in a controlled and efficient manner, offering potential benefits across a wide spectrum of applications.

Microflakes composed of mixed cerium molybdenum oxide hydrates were synthesized from soluble precursors and co-deposited with a nickel matrix to form Ni–Ce,Mo oxide composite coatings [72]. It was concluded that DES-assisted electroplating solutions made it possible to successfully prepare composite layers, resulting in nanocrystalline Ni matrices with a smaller crystallite size compared to the pure nickel electrodeposits (6.3 nm and 10.4 nm, respectively). The corrosion behavior of these composite coatings in an aggressive 0.05 M NaCl solution was extensively investigated. During corrosion, NiO changed into Ni(OH)<sub>2</sub>, whereas oxides of molybdenum were removed from the coating surface. These findings hold potential interest in creating novel surface films exhibiting self-healing behavior.

An interesting approach to the electrodeposition of composite coatings involves the co-deposition of a metallic matrix with metallic particles of a dispersed phase. For instance, the patterns of electrodeposition and the properties of the resulting composites from electrolytes based on DESs containing dissolved nickel (II) salt and nanoparticles of titanium or aluminum have been investigated [73,74]. Specifically, the titanium content in a composite coating depends on the concentration of particles in the electrolyte, current density, and duty cycle when using pulse electrolysis, and can reach approximately 11 wt.% [73]. Here, a DES (ethaline) with different loadings of titanium nanoparticles (4, 8, 16, or 32 g L<sup>-1</sup>) was used. The adsorption and incorporation of titanium particles significantly altered the nucleation conditions of the nickel. Indeed, the nucleation for pure Ni originally followed a three-dimensional progressive mechanism, which then gradually shifted towards a three-dimensional instantaneous model as the applied electrode potential became more negative. At the same time, the nucleation of the nickel matrix in the Ni–Ti composites corresponded to the three-dimensional instantaneous model initially but progressively ceased to obey simple theoretical models. The resulting Ni–Ti nanostructured composite films had enhanced corrosion stability, which further improved with the increase in Ti nanoparticle loading. Therefore, this approach was anticipated to produce high-performance nickel–titanium nanocomposite layers with excellent anti-corrosion performance.

The aluminum content in a composite coating deposited using an electrolyte on a DES was found to reach nearly 20 wt.% [74]. In this study, the content of Al nanoparticles in the DES-based colloidal plating baths was 4, 8, 16, or 32 g L<sup>-1</sup>. The embedded aluminum nanoparticles in the DES-based plating baths facilitated the electrodeposition of Ni(II) complex ions, causing the nucleation mechanism to significantly deviate from the three-dimensional instantaneous mechanism. Nickel–aluminum composite electrodeposits revealed a slight decrease in the microhardness and anticorrosion properties compared with nickel coatings. Nevertheless, the incorporation of aluminum particulates notably enhanced the anti-oxidation ability of the composite layers. Furthermore, a high-temperature thermal treatment resulted in the formation of NiAl intermetallic and different oxides, which improved the microhardness and corrosion stability. The suggested process of Ni–Al composite fabrication is promising for the creation of anti-corrosion and high-strength surface films.

Composite coatings can be formed with a matrix not only based on “pure” individual metals but also from electrodeposited metal alloys. However, due to the apparent complexity of such processes, there have been relatively few studies in this area. In particular, a single study [75] has been published investigating the incorporation of reduced graphene oxide particles into an electrodeposited matrix of the nickel alloy NiSn (NiSn-rGO composite) using an ethaline-based electrolyte. Under pulse current conditions, high-quality NiSn-rGO composite films were cathodically deposited, exhibiting satisfactory adhesion to the copper substrate. The incorporation of graphene oxide sheets into the nickel–tin

alloy affected the patterns of surface profile, grain size, and roughness of surface. Notably, an enhancement in corrosion resistance was observed for the NiSn-rGO composites in comparison to the pure nickel–tin alloy.

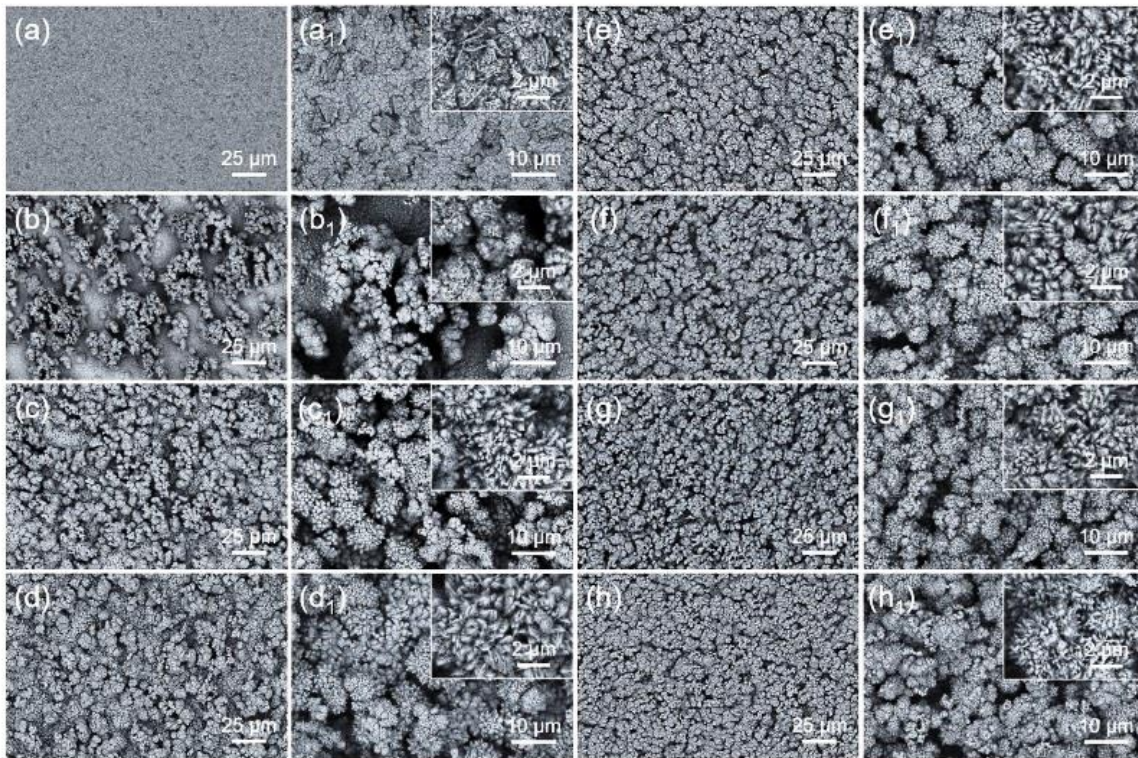


**Figure 11.** SEM microphotographs of nickel–nano-carbon composite coatings deposited with various contents of carbon nanoparticles in solution (g/L): 0 (**a,a<sub>1</sub>**), 0.1 (**b,b<sub>1</sub>**), 0.2 (**c,c<sub>1</sub>**), 0.3 (**d,d<sub>1</sub>**), 0.4 (**e,e<sub>1</sub>**), 0.5 (**f,f<sub>1</sub>**), 0.6 (**g,g<sub>1</sub>**), and 0.7 (**h,h<sub>1</sub>**). The insets correspond to higher magnification of SEM microphotographs. Reprinted from [69], copyright 2019, with permission from Elsevier.

It should be noted that the electrochemical deposition of composite coatings from DESs that contain a metallic dispersed phase and/or a matrix not of pure metal but an alloy of multiple metals represents one of the most intriguing and promising directions. Clearly, this conclusion applies to deposited composites not only based on nickel but also based on other metals.

### 3.6. Cobalt-Based Composites

Electrodeposited composite films composed of a cobalt matrix with incorporated multiwalled carbon nanotubes were fabricated utilizing a reline-based deep eutectic solvent (a mixture of urea and choline chloride) [76]. The molar concentration of  $\text{CoCl}_2 \cdot 6\text{H}_2\text{O}$  in the electrolytes was  $1 \text{ mol L}^{-1}$  and the content of the MWCNTs was in the range of 0.1 to  $0.5 \text{ g L}^{-1}$ . The resulting coatings of cobalt and cobalt–MWCNTs composites exhibited a uniform and smooth surface, demonstrating excellent adhesion to the Cu substrates. X-ray diffraction analysis revealed that the inclusion of MWCNTs induced a preferential orientation of metal crystallites along the (220) plane, indicating the grain refinement effect of the multiwalled carbon nanotubes. In contrast to the sharp-edged grain structure observed in pure cobalt deposits, the cobalt-based composites displayed a less dense formation characterized by relatively spherical particles interconnected by MWCNTs. It was noted that the incorporation of MWCNTs led to a reduction in the surface roughness of the electrodeposits. The corrosion resistance of the cobalt–MWCNT composite films was found to be comparable and, in some cases, slightly superior to that of pure cobalt layers, particularly evident during prolonged exposure to a 0.5 M NaCl solution. These improved

corrosion properties were attributed to the hindrance of aggressive chloride ions' diffusion by the MWCNTs.

### 3.7. Chromium-Based Composites

The pulse electrodeposition synthesis and characterization of chromium–single-walled carbon nanotube (Cr–SWCNT) composite coatings have been reported [77]. An environmentally safe Cr(III) plating bath was employed containing dissolved chromium chloride, choline chloride, sodium chloride, ethylene glycol, and single-walled carbon nanotubes with diameters typically below 2 nm and lengths ranging from 5 to 15  $\mu\text{m}$ . An exceptional current efficiency of approximately 70% was achieved for the Cr–SWCNT composite electroplating, representing a significant improvement compared to the typical 10%–20% current efficiency observed in industrial Cr(VI) plating baths [78]. The resulting composite coatings exhibited a uniform and crack-free surface morphology, with embedded SWCNTs forming bundles that were incorporated into the chromium metal matrix as aggregates [77]. The electroplated Cr–SWCNT composites displayed notably enhanced microhardness, measuring around 540 HV compared to the approximate 280 HV of pure chromium. Corrosion electrochemical behavior was studied in a 3.5% NaCl water solution, and the results revealed that the composite Cr–SWCNT coatings exhibited superior anti-corrosive properties in comparison to pure Cr layers.

Mejía-Caballero et al. [79] investigated the mechanisms governing the nucleation and diffusion-controlled growth of Cr nanosized particles on a glassy carbon rotating disk electrode using an ethaline-based electrolyte in which 50 mM Cr(III) ions were dissolved in the form of  $\text{CrCl}_3 \cdot 6\text{H}_2\text{O}$  salt. The resulting coating, in addition to metallic chromium, also contained particles of  $\text{Cr}(\text{OH})_3$  and  $\text{Cr}_2\text{O}_3$  compounds, thus categorizing it as a composite material. The formation of trivalent chromium oxide–hydroxide phases was attributed to the interaction with hydroxide ions, which were generated as a result of the electrochemical reduction of residual water. Consequently, the electrodeposited nanoparticles displayed a core–shell microstructure, with the core comprising metallic, zero-valent Cr and the shell consisting of trivalent chromium compounds in the form of  $\text{Cr}_2\text{O}_3$  and  $\text{Cr}(\text{OH})_3$ . Unfortunately, no physicochemical properties of the synthesized composite coating were investigated.

## 4. Conclusions and Possible Directions of Future Research

The electroplating of composite coatings stands as a remarkably potent and versatile technique for markedly enhancing the physicochemical and operational characteristics of surfaces, thereby imparting augmented functional properties. The scrutinized literature underscores that the electrochemical synthesis of composites facilitates the development of surface layers with heightened resistance against corrosion and wear, elevated microhardness, and distinctive electrocatalytic and photocatalytic properties. Diverse categories of plating baths can be utilized for the electrochemical deposition of composite coatings, with aqueous solutions retaining widespread usage. Nonetheless, the usage of aqueous solutions is not devoid of shortcomings; they are susceptible to aggregation and sedimentation processes, thereby compromising the stability of the bath composition and the electroplating process. One possible solution to this problem is the implementation of non-aqueous plating baths, with solutions based on deep eutectic solvents being particularly promising in this context.

Plating baths involving deep eutectic solvents present notable benefits, characterized by their environmental friendliness, ease of access, and cost-effectiveness concerning primary constituents and synthesis techniques. These baths further provide enhanced colloidal and sedimentation stability for electrolytes, facilitating the deposition of coatings featuring a diverse spectrum of precisely controlled phases and chemical compositions. Such achievements often remain elusive when employing aqueous electrolytes or plating solutions based on organic solvents. Moreover, there exists versatility in fine-tuning the properties of electrolytes based on DESs and the characteristics of the coatings deposited

using these solutions. This flexibility enables precise control over the composition, structure, and properties of the coatings, ensuring tailored performance for diverse applications.

In this review, literature data on the kinetics and mechanisms of co-deposition, as well as the key operational characteristics of the composite electrodeposits obtained from DES-based plating electrolytes, were systematically examined for the first time.

Highlighting the critical avenues for future research, the exploration of the electrodeposition of composite coatings from electrolytes formulated with deep eutectic solvents necessitates attention towards the following key directions:

1. Refinement of electrolyte compositions. A paramount objective lies in the meticulous adjustment of electrolyte compositions. This involves an in-depth investigation into the influence of diverse constituents within DES-based electrolytes, aiming to optimize their composition for the enhancement of composite coating properties.
2. Investigation of nanoparticle size effects. Establishing discernible patterns concerning the impact of nanoparticle sizes assumes significance. It is imperative to delve into the effects of varying sizes of nanoparticles within the dispersed phase on the kinetics and inherent properties of electrochemically deposited composite coatings. This avenue of research should provide insights into the interaction between nanoparticle dimensions and the resulting coating characteristics, paving the way for tailored coatings with precise functionalities.
3. Exploration of co-deposition mechanisms. A thorough investigation into the electrodeposition mechanism is essential to the advancement of knowledge in this field. This involves a comprehensive exploration of the interactions between the electrochemical processes, adsorption kinetics at the electrode surface, and the resulting microstructure and chemical composition of composite coatings. Such in-depth studies should reveal the underlying mechanisms governing the formation of these coatings, offering insights into optimizing the deposition process for enhanced performance.
4. Analysis of colloidal–chemical behavior of DES-based electrolytes. A crucial aspect of future research involves establishing clear patterns in the colloidal–chemical behavior of suspensions and colloidal electrolytes formulated with DESs. These electrolytes are pivotal for the electrolytic deposition of composite films. The goal is to develop more stable and reliable technological processes tailored for practical applications. Understanding the behavior of these systems at a molecular level will enable the fine-tuning of deposition parameters, leading to improved coating quality and durability.
5. Utilization of advanced characterization techniques. The application of advanced characterization methods, such as in situ monitoring or real-time imaging, holds particular significance for a comprehensive understanding of the evolution of composite coatings during electrodeposition. These cutting-edge techniques should offer invaluable insights into the dynamic processes occurring at the electrode interface, allowing for precise observations of morphological changes, phase transformations, and surface interactions in real time. Such detailed analysis will aid in elucidating the mechanisms governing the formation of composite coatings, thereby paving the way for optimized deposition strategies and enhanced coating properties.
6. Identifying pathways for the flexible control of process parameters. This involves the identification of pathways for flexible control over process parameters. Specifically, it is of great value to delve into the effects of various parameters such as temperature, stirring rates, current densities, and different current regimes on the deposition kinetics and resultant properties of composite coatings. By systematically varying these parameters and analyzing their impact on coating morphology, composition, and performance, optimized process conditions tailored to specific application requirements could be established. This endeavor should aim to uncover the interactions between process variables and coating characteristics, facilitating the development of advanced and adaptable electrodeposition techniques for composite coatings.
7. Tailoring specific composites for targeted applications. A pivotal focus for future research lies in the development of tailored composites designed for specific appli-

cations. This involves meticulous adjustments to the composition, structure, and properties of coatings to align with the requirements of distinct end-use scenarios. Of notable promise and significance is the advancement of high-performance, reliable electrocatalysts tailored for use in green hydrogen energy applications. By fine-tuning the characteristics of these coatings, researchers aim to enhance efficiency, durability, and overall performance for sustainable energy processes.

8. Integration of environmental and economic considerations. It is imperative to incorporate mandatory evaluations of environmental sustainability and economic feasibility. This aspect holds particular weight when employing DES-based electrolytes, necessitating the exploration of eco-friendly and cost-effective approaches. Understanding the environmental footprint and economic viability of these processes ensures the development of sustainable practices that align with global initiatives towards greener technologies.
9. Exploration of multi-elemental and multi-phase composite deposition. A promising frontier emerges in the field of multi-elemental and multi-phase composite deposition. This direction extends the research horizon to encompass the simultaneous deposition of multiple elements or compounds within composite coatings. This innovative approach not only expands the range of functionalities but also offers enhanced versatility and performance in various technological applications.

**Funding:** This research was funded by the Ministry of Education and Science of Ukraine, grant number 0124U000563.

**Institutional Review Board Statement:** Not applicable.

**Informed Consent Statement:** Not applicable.

**Data Availability Statement:** The data presented in this study are available upon request from the corresponding author. The data are not publicly available due to technical limitations.

**Conflicts of Interest:** The author declares no conflicts of interest. The funders had no role in the design of the study; in the collection, analyses, or interpretation of data; in the writing of the manuscript; or in the decision to publish the results.

## References

1. Okonkwo, B.O.; Jeong, C.; Jang, C. Advances on Cr and Ni electrodeposition for industrial applications—A review. *Coatings* **2022**, *12*, 1555. [[CrossRef](#)]
2. Larson, C.; Smith, J.R. Recent trends in metal alloy electrolytic and electroless plating research: A review. *Trans. Inst. Mater. Finish.* **2011**, *89*, 333–341. [[CrossRef](#)]
3. Schlesinger, M.; Paunovic, M. *Modern Electroplating*, 5th ed.; John Wiley & Sons: Hoboken, NJ, USA, 2014; 752p.
4. Walsh, F.C.; Wang, S.; Zhou, N. The electrodeposition of composite coatings: Diversity, applications and challenges. *Curr. Opin. Electrochem.* **2020**, *20*, 8–19. [[CrossRef](#)]
5. Walsh, F.C.; Larson, C. Towards improved electroplating of metal-particle composite coatings. *Trans. Inst. Mater. Finish.* **2020**, *98*, 288–299. [[CrossRef](#)]
6. Low, C.T.J.; Wills, R.G.A.; Walsh, F.C. Electrodeposition of composite coatings containing nanoparticles in a metal deposit. *Surf. Coat. Technol.* **2006**, *201*, 371–383. [[CrossRef](#)]
7. Walsh, F.C.; Ponce de Leon, C. A review of the electrodeposition of metal matrix composite coatings by inclusion of particles in a metal layer: An established and diversifying technology. *Trans. Inst. Mater. Finish.* **2014**, *92*, 83–98. [[CrossRef](#)]
8. Musiani, M. Electrodeposition of composites: An expanding subject in electrochemical materials science. *Electrochim. Acta* **2000**, *45*, 3397–3402. [[CrossRef](#)]
9. Smith, E.L.; Abbott, A.P.; Ryder, K.S. Deep eutectic solvents (DESs) and their applications. *Chem. Rev.* **2014**, *114*, 11060–11082. [[CrossRef](#)] [[PubMed](#)]
10. Zhang, Q.; Vigier, K.D.O.; Royer, S.; Jérôme, F. Deep eutectic solvents: Syntheses, properties and applications. *Chem. Soc. Rev.* **2012**, *41*, 7108–7146. [[CrossRef](#)] [[PubMed](#)]
11. Hansen, B.B.; Spittle, S.; Chen, B.; Poe, D.; Zhang, Y.; Klein, J.M.; Horton, A.; Adhikari, L.; Zelovich, T.; Doherty, B.W.; et al. Deep eutectic solvents: A review of fundamentals and applications. *Chem. Rev.* **2021**, *121*, 1232–1285. [[CrossRef](#)] [[PubMed](#)]
12. Abbott, A.P.; Edler, K.J.; Page, A.J. Deep eutectic solvents—The vital link between ionic liquids and ionic solutions. *J. Chem. Phys.* **2021**, *155*, 150401. [[CrossRef](#)]

13. Tome, L.I.N.; Baiao, V.; da Silva, W.; Brett, C.M.A. Deep eutectic solvents for the production and application of new materials. *Appl. Mater. Today* **2018**, *10*, 30–50. [[CrossRef](#)]
14. Abbott, A.P.; Ryder, K.S.; König, U. Electrofinishing of metals using eutectic based ionic liquids. *Trans. Inst. Mater. Finish.* **2008**, *86*, 196–204. [[CrossRef](#)]
15. Smith, E.L. Deep eutectic solvents (DESs) and the metal finishing industry: Where are they now? *Trans. Inst. Mater. Finish.* **2013**, *91*, 241–248. [[CrossRef](#)]
16. Abbott, A.P. Deep eutectic solvents and their application in electrochemistry. *Curr. Opin. Green Sustain. Chem.* **2022**, *36*, 100649. [[CrossRef](#)]
17. Costa, J.G.d.R.d.; Costa, J.M.; Almeida Neto, A.F.d. Progress on electrodeposition of metals and alloys using ionic liquids as electrolytes. *Metals* **2022**, *12*, 2095. [[CrossRef](#)]
18. Liu, Y.; Deak, N.; Wang, Z.; Yu, H.; Hameleers, L.; Jurak, E.; Deuss, P.J.; Barta, K. Tunable and functional deep eutectic solvents for lignocellulose valorization. *Nat. Commun.* **2021**, *12*, 5424. [[CrossRef](#)] [[PubMed](#)]
19. Sanches, M.V.; Freitas, R.; Oliva, M.; Mero, A.; De Marchi, L.; Cuccaro, A.; Fumagalli, G.; Mezzetta, A.; Colombo Dugoni, G.; Ferro, M.; et al. Are natural deep eutectic solvents always a sustainable option? A bioassay-based study. *Environ. Sci. Pollut. Res.* **2023**, *30*, 17268–17279. [[CrossRef](#)]
20. Haerens, K.; Matthijs, E.; Chmielarz, A.; Van der Bruggen, B. The use of ionic liquids based on choline chloride for metal deposition: A green alternative? *J. Environ. Manag.* **2009**, *90*, 3245–3252. [[CrossRef](#)]
21. Nam, N.N.; Do, H.D.K.; Trinh, K.T.L.; Lee, N.Y. Design strategy and application of deep eutectic solvents for green synthesis of nanomaterials. *Nanomaterials* **2023**, *13*, 1164. [[CrossRef](#)] [[PubMed](#)]
22. Kityk, A.; Pavlik, V.; Hnatko, M. Exploring deep eutectic solvents for the electrochemical and chemical synthesis of photo and electrocatalysts for hydrogen evolution. *Int. J. Hydrogen Energy* **2023**, *48*, 39823–39853. [[CrossRef](#)]
23. Danilov, F.I.; Protsenko, V.S. Electrodeposition of composite coatings using electrolytes based on deep eutectic solvents: A mini-review. *Vopr. Khimii i Khimicheskoi Tekhnologii* **2018**, 13–21.
24. Abbott, A.P.; El Ttaib, K.; Frisch, G.; McKenzie, K.J.; Ryder, K.S. Electrodeposition of copper composites from deep eutectic solvents based on choline chloride. *Phys. Chem. Chem. Phys.* **2009**, *11*, 4269–4277. [[CrossRef](#)] [[PubMed](#)]
25. Higashitani, K.; Kondo, M.; Hatade, S. Effect of particle size on coagulation rate of ultrafine colloidal particles. *J. Colloid Interface Sci.* **1991**, *142*, 204–213. [[CrossRef](#)]
26. Shchukin, E.D.; Pertsov, A.V.; Amelina, E.A.; Zelenev, A.S. *Colloid and Surface Chemistry*; Elsevier: Amsterdam, The Netherlands, 2001.
27. You, Y.-H.; Gu, C.-D.; Wang, X.-L.; Tu, J.-P. Electrochemical preparation and characterization of Ni-PTFE composite coatings from a non-aqueous solution without additives. *Int. J. Electrochem. Sci.* **2012**, *7*, 12440–12455. [[CrossRef](#)]
28. Li, R.; Hou, Y.; Liu, B.; Wang, D.; Liang, J. Electrodeposition of homogenous Ni/SiO<sub>2</sub> nanocomposite coatings from deep eutectic solvent with in-situ synthesized SiO<sub>2</sub> nanoparticles. *Electrochim. Acta* **2016**, *222*, 1272–1280. [[CrossRef](#)]
29. Li, R.; Hou, Y.; Liang, J. Electro-codeposition of Ni-SiO<sub>2</sub> nanocomposite coatings from deep eutectic solvent with improved corrosion resistance. *Appl. Surf. Sci.* **2016**, *367*, 449–458. [[CrossRef](#)]
30. Guglielmi, N. Kinetics of the deposition of inert particles from electrolytic baths. *J. Electrochem. Soc.* **1972**, *119*, 1009–1012. [[CrossRef](#)]
31. Celis, J.P.; Roos, J.R.; Buelens, C. A mathematical model for the electrolytic codeposition of particles with a metallic matrix. *J. Electrochem. Soc.* **1987**, *134*, 1402–1408. [[CrossRef](#)]
32. Franssaer, J.; Celis, J.P.; Roos, J.R. Analysis of the electrolytic codeposition of non-Brownian particles with metals. *J. Electrochem. Soc.* **1992**, *139*, 413–425. [[CrossRef](#)]
33. Maurin, G.; Lavanant, A. Electrodeposition of nickel/silicon carbide composite coatings on a rotating disc electrode. *J. Appl. Electrochem.* **1995**, *25*, 1113–1121. [[CrossRef](#)]
34. Hwang, B.J.; Hwang, C.S. Mechanism of codeposition of silicon carbide with electrolytic cobalt. *J. Electrochem. Soc.* **1993**, *140*, 979–984. [[CrossRef](#)]
35. Vereecken, P.M.; Shao, I.; Searson, P.C. Particle codeposition in nanocomposite films. *J. Electrochem. Soc.* **2000**, *147*, 2572–2575. [[CrossRef](#)]
36. Shao, I.; Vereecken, P.M.; Cammarata, R.C.; Searson, P.C. Kinetics of particle codeposition of nanocomposite. *J. Electrochem. Soc.* **2002**, *149*, C610–C614. [[CrossRef](#)]
37. Berçot, P.; Peña-Muñoz, E.; Pagetti, J. Electrolytic composite Ni-PTFE coatings: An adaptation of Guglielmi's model for the phenomena of incorporation. *Surf. Coat. Technol.* **2002**, *157*, 282–289. [[CrossRef](#)]
38. Bahadormanesh, B.; Dolati, A. The kinetics of Ni-Co/SiC composite coatings electrodeposition. *J. Alloys Compd.* **2010**, *504*, 514–518. [[CrossRef](#)]
39. Eroglu, D.; West, A.C. Mathematical modeling of Ni/SiC co-deposition in the presence of a cationic dispersant. *J. Electrochem. Soc.* **2013**, *160*, D354–D360. [[CrossRef](#)]
40. Adamczyk, Z.; Jaszółt, K.; Michna, A.; Siwek, B.; Szyk-Warszyńska, L.; Zembala, M. Irreversible adsorption of particles on heterogeneous surfaces. *Adv. Colloid Interface Sci.* **2005**, *118*, 25–42. [[CrossRef](#)]
41. Wojtaszczyk, P.; Bonet Avalos, J.; Rubi, J.M. Kinetics of particles adsorption processes driven by diffusion. *Europhys. Lett.* **1997**, *40*, 299–304. [[CrossRef](#)]
42. Binks, B.P. Particles as surfactants—Similarities and differences. *Curr. Opin. Colloid Interface Sci.* **2002**, *7*, 21–41. [[CrossRef](#)]

43. Protsenko, V.S.; Danilov, F.I. Kinetic model of composite coatings electrodeposition assuming irreversible adsorption of dispersed particles on a growing metal substrate. *J. Electroanal. Chem.* **2022**, *918*, 116463. [[CrossRef](#)]
44. Atilhan, M.; Aparicio, S. Deep eutectic solvents on the surface of face centered cubic metals. *J. Phys. Chem. C* **2016**, *120*, 10400–10409. [[CrossRef](#)]
45. Mamme, M.H.; Moors, S.L.C.; Terry, H.A.; Deconinck, J.; Ustarroz, J.; De Proft, F. Atomistic insights into the electrochemical double layer of choline chloride-urea deep eutectic solvent: A clustered interfacial structuring. *J. Phys. Chem. Lett.* **2018**, *9*, 6296–6304. [[CrossRef](#)] [[PubMed](#)]
46. Danilov, F.I.; Kityk, A.A.; Shaiderov, D.A.; Bogdanov, D.A.; Korniy, S.A.; Protsenko, V.S. Electrodeposition of Ni–TiO<sub>2</sub> composite coatings using electrolyte based on a deep eutectic solvent. *Surf. Eng. Appl. Electrochem.* **2019**, *55*, 138–149. [[CrossRef](#)]
47. Bobrova, L.S.; Danilov, F.I.; Protsenko, V.S. Effects of temperature and water content on physicochemical properties of ionic liquids containing CrCl<sub>3</sub>·xH<sub>2</sub>O and choline chloride. *J. Mol. Liq.* **2016**, *223*, 48–53. [[CrossRef](#)]
48. Protsenko, V.S.; Bogdanov, D.A.; Korniy, S.A.; Kityk, A.A.; Baskevich, A.S.; Danilov, F.I. Application of a deep eutectic solvent to prepare nanocrystalline Ni and Ni/TiO<sub>2</sub> coatings as electrocatalysts for the hydrogen evolution reaction. *Int. J. Hydrogen Energy* **2019**, *44*, 24604–24616. [[CrossRef](#)]
49. Li, R.; Chu, Q.; Liang, J. Electrodeposition and characterization of Ni–SiC composite coatings from deep eutectic solvent. *RSC Adv.* **2015**, *5*, 44933–44942. [[CrossRef](#)]
50. El Ttaib, K.; Benhmid, A. The study of the effect of surfactants on copper codeposition with SiC nano particulate from deep eutectic solvent ionic liquids (Ethaline). *Int. Res. J. Pure Appl. Chem.* **2024**, *25*, 22–27. [[CrossRef](#)]
51. Abbott, A.P.; El Ttaib, K.; Frisch, G.; Ryder, K.S.; Weston, D. The electrodeposition of silver composites using deep eutectic solvents. *Phys. Chem. Chem. Phys.* **2012**, *14*, 2443–2449. [[CrossRef](#)]
52. Marín-Sánchez, M.; Gracia-Escosa, E.; Conde, A.; Palacio, C.; García, I. Deposition of zinc–cerium coatings from deep eutectic ionic liquids. *Materials* **2018**, *11*, 2035. [[CrossRef](#)]
53. Li, R.; Liang, J.; Hou, Y.; Chu, Q. Enhanced corrosion performance of Zn coating by incorporating graphene oxide electrodeposited from deep eutectic solvent. *RSC Adv.* **2015**, *5*, 60698–60707. [[CrossRef](#)]
54. Costovici, S.; Pantazi, A.; Balan, D.; Cojocar, A.; Visan, T.; Enachescu, M.; Anicai, L. Electrodeposition of tin-reduced graphene oxide composite from deep eutectic solvents based on choline chloride and ethylene glycol. *Metals* **2023**, *13*, 203. [[CrossRef](#)]
55. Protsenko, V.S.; Butyrina, T.E.; Bogdanov, D.A.; Korniy, S.A.; Danilov, F.I. Electrochemical synthesis of Ni/TiO<sub>2</sub> composite coatings from deep eutectic solvent and electrocatalytic characteristics of deposits. *Surf. Eng. Appl. Electrochem.* **2022**, *58*, 440–450. [[CrossRef](#)]
56. Protsenko, V.S.; Butyrina, T.E.; Bobrova, L.S.; Korniy, S.A.; Danilov, F.I. Electrochemical corrosion behavior of Ni–TiO<sub>2</sub> composite coatings electrodeposited from a deep eutectic solvent-based electrolyte. *Coatings* **2022**, *12*, 800. [[CrossRef](#)]
57. Protsenko, V.S.; Butyrina, T.E.; Bobrova, L.S.; Danilov, F.I. Preparation and characterization of Ni–TiO<sub>2</sub> composites electrodeposited from an ethylene glycol-based deep eutectic solvent. *Mater. Today Proc.* **2022**, *62*, 7712–7716. [[CrossRef](#)]
58. Danilov, F.I.; Protsenko, V.S.; Kityk, A.A.; Shaiderov, D.A.; Vasil'eva, E.A.; Pramod Kumar, U.; Joseph Kennady, C. Electrodeposition of nanocrystalline nickel coatings from a deep eutectic solvent with water addition. *Prot. Met. Phys. Chem. Surf.* **2017**, *53*, 1131–1138. [[CrossRef](#)]
59. Gu, C.D.; You, Y.H.; Yu, Y.L.; Qu, S.X.; Tu, J.P. Microstructure, nanoindentation, and electrochemical properties of the nanocrystalline nickel film electrodeposited from choline chloride–ethylene glycol. *Surf. Coat. Technol.* **2011**, *205*, 4928–4933. [[CrossRef](#)]
60. Abbott, A.P.; El Ttaib, K.; Ryder, K.S.; Smith, E.L. Electrodeposition of nickel using eutectic based ionic liquids. *Trans. Inst. Mater. Finish.* **2008**, *86*, 234–240. [[CrossRef](#)]
61. Osman, A.I.; Mehta, N.; Elgarahy, A.M.; Hefny, M.; Al-Hinai, A.; Al-Muhtaseb, A.H.; Rooney, D.W. Hydrogen production, storage, utilisation and environmental impacts: A review. *Environ. Chem. Lett.* **2022**, *20*, 153–188. [[CrossRef](#)]
62. Farias, C.B.B.; Barreiros, R.C.S.; da Silva, M.F.; Casazza, A.A.; Converti, A.; Sarubbo, L.A. Use of hydrogen as fuel: A trend of the 21st century. *Energies* **2022**, *15*, 311. [[CrossRef](#)]
63. Ahmad, R.; Ahmad, Z.; Khan, A.U.; Mastoi, N.R.; Aslam, M.; Kim, J. Photocatalytic systems as an advanced environmental remediation: Recent developments, limitations and new avenues for applications. *J. Environ. Chem. Eng.* **2016**, *4*, 4143–4164. [[CrossRef](#)]
64. Shan, A.Y.; Ghazi, T.I.M.; Rashid, S.A. Immobilisation of titanium dioxide onto supporting materials in heterogeneous photocatalysis: A review. *Appl. Catal. A Gen.* **2010**, *389*, 1–8. [[CrossRef](#)]
65. Liu, S.; Ji, R.; Liu, Y.; Zhang, F.; Jin, H.; Li, X.; Zheng, Q.; Lu, S.; Cai, B. Effects of boric acid and water on the deposition of Ni/TiO<sub>2</sub> composite coatings from deep eutectic solvent. *Surf. Coat. Technol.* **2021**, *409*, 126834. [[CrossRef](#)]
66. Martis, P.; Dilimon, V.S.; Delhalle, J.; Mekhalif, Z. Electro-generated nickel/carbon nanotube composites in ionic liquid. *Electrochim. Acta* **2010**, *55*, 5407–5410. [[CrossRef](#)]
67. Liu, D.G.; Sun, J.; Gui, Z.X.; Song, K.J.; Luo, L.M.; Wu, Y.C. Super-low friction nickel based carbon nanotube composite coating electro-deposited from eutectic solvents. *Diamond Relat. Mater.* **2017**, *74*, 229–232. [[CrossRef](#)]
68. Xiang, L.; Shen, Q.; Zhang, Y.; Bai, W.; Nie, C. One-step electrodeposited Ni-graphene composite coating with excellent tribological properties. *Surf. Coat. Technol.* **2019**, *373*, 38–46. [[CrossRef](#)]

69. Wang, S.; Zou, X.; Shi, T.; Ding, K.; Pang, Z.; Huang, Y.; Tang, W.; Xu, Q.; Zhou, Z.; Lu, X. Facile electrodeposition of three-dimensional flower-like structure of nickel matrix composite electrodes for hydrogen evolution reaction. *Appl. Surf. Sci.* **2019**, *498*, 143768. [[CrossRef](#)]
70. Zubar, T.I.; Fedosyuk, V.M.; Trukhanov, A.V.; Kovaleva, N.N.; Astapovich, K.A.; Vinnik, D.A.; Trukhanova, E.L.; Kozlovskiy, A.L.; Zdorovets, M.V.; Solobai, A.A.; et al. Control of growth mechanism of electrodeposited nanocrystalline NiFe films. *J. Electrochem. Soc.* **2019**, *166*, D173–D180. [[CrossRef](#)]
71. Cherigui, E.A.M.; Sentosun, K.; Bouckenooge, P.; Vanrompay, H.; Bals, S.; Terryn, H.; Ustarroz, J. Comprehensive study of the electrodeposition of nickel nanostructures from deep eutectic solvents: Self-limiting growth by electrolysis of residual water. *J. Phys. Chem. C* **2017**, *121*, 9337–9347. [[CrossRef](#)]
72. Winiarski, J.; Niciejewska, A.; Ryl, J.; Darowicki, K.; Baśladyńska, S.; Winiarska, K.; Szczygieł, B. Ni/cerium molybdenum oxide hydrate microflakes composite coatings electrodeposited from choline chloride: Ethylene glycol deep eutectic solvent. *Materials* **2020**, *13*, 924. [[CrossRef](#)] [[PubMed](#)]
73. Hou, Y.; Peng, Z.; Liang, J.; Fu, S. Ni–Ti nanocomposite coatings electro-codeposited from deep eutectic solvent containing Ti nanoparticles. *J. Electrochem. Soc.* **2020**, *167*, 042502. [[CrossRef](#)]
74. Hou, Y.; Peng, Z.; Liang, J.; Liu, M. Ni–Al nanocomposite coating electrodeposited from deep eutectic solvent. *Surf. Coat. Technol.* **2021**, *405*, 126587. [[CrossRef](#)]
75. Rosoiu, S.P.; Pantazi, A.G.; Petica, A.; Cojocaru, A.; Costovici, S.; Zanella, C.; Visan, T.; Anicai, L.; Enachescu, M. Electrodeposition of NiSn-rGO composite coatings from deep eutectic solvents and their physicochemical characterization. *Metals* **2020**, *10*, 1455. [[CrossRef](#)]
76. Pereira, N.M.; Brincoveanu, O.; Pantazi, A.G.; Pereira, C.M.; Araújo, J.P.; Silva, A.F.; Enachescu, M.; Anicai, L. Electrodeposition of Co and Co composites with carbon nanotubes using choline chloride-based ionic liquids. *Surf. Coat. Technol.* **2017**, *324*, 451–462. [[CrossRef](#)]
77. Maharaja, J.; Raja, M.; Mohan, S. Pulse electrodeposition of Cr–SWCNT composite from choline chloride based electrolyte. *Surf. Eng.* **2014**, *30*, 722–727. [[CrossRef](#)]
78. Protsenko, V.S. Kinetics and mechanism of electrochemical reactions occurring during the chromium electrodeposition from electrolytes based on Cr(III) compounds: A literature review. *Reactions* **2023**, *4*, 398–419. [[CrossRef](#)]
79. Mejía-Caballero, I.; Le Manh, T.; Aldana-González, J.; Arce-Estrada, E.M.; Romero-Romo, M.; Campos-Silva, I.; Ramírez-Silva, M.T.; Palomar-Pardavé, M. Electrodeposition of nanostructured chromium conglomerates from Cr(III) dissolved in a deep eutectic solvent: Influence of forced convection. *J. Electrochem. Soc.* **2021**, *168*, 112512. [[CrossRef](#)]

**Disclaimer/Publisher’s Note:** The statements, opinions and data contained in all publications are solely those of the individual author(s) and contributor(s) and not of MDPI and/or the editor(s). MDPI and/or the editor(s) disclaim responsibility for any injury to people or property resulting from any ideas, methods, instructions or products referred to in the content.